

# Layer-by-layer modified anion-exchange membranes for phosphate recovery

by

Arvind Dwarkasing

A thesis submitted in partial fulfillment  
of the requirements for the degree

of

MASTER OF SCIENCE

in

Applied Physics

---

Professor:  
Prof. dr. E.J.R. Sudhölter

---

Supervisors:  
Laura Paltrinieri, MSc.  
Dr. Lukasz Poltorak

DELFT UNIVERSITY OF TECHNOLOGY

August 9, 2017

## Abstract

Ion exchange membranes (IEMs) are used to selectively transport ions between two solutions. Most membranes are not selective to certain ion species. This study investigates the possibility of increasing phosphate selectivity (in the form of  $\text{H}_2\text{PO}_4^-$ ) of anion exchange membranes (AEM) by modifying commercial AEMs with a Layer-by-Layer (LbL) assembly of a few promising candidate polyelectrolytes (PE): Poly(diallyldimethylammonium chloride) (PDADMAC), poly(allylamine hydrochloride) (PAH), and poly(allylamine hydrochloride)-Guanidinium (PAH-Gu). The anionic layer was composed of poly(sodium 4-styrene sulfonate) (PSS). Membranes were modified with 4 layers. This was done on only one side, the asymmetric modification  $((\text{PE}/\text{PSS})_4)$ , or both sides of the membrane, the symmetric modification  $((\text{PE}/\text{PSS})_2)$ . The membranes were then characterized using low-frequency impedance spectroscopy to obtain, among other parameters, the resistance of the membrane.

Asymmetrically modified membranes showed non-reproducible impedance data, while their symmetric counterpart was in good agreement with a theoretical model. Compared to the bare membrane, a decrease in the membrane's resistivity was found for all the modified membranes in the studied salt concentrations (0.1 to 0.4 M). In the low concentration region, the PAH-Gu modified membrane had the lowest resistance. This result is most likely caused by a high affinity between Guanidinium and phosphate. The electric properties of other parameters, such as diffusive boundary layer and electrical double layer resistance, were found to be independent from the membrane modification.

We then performed permselectivity measurements with a competing anion, sulfate. To this end, electrodialysis was performed in the underlimiting current regime. Modified membranes showed no increase in discriminatory function for phosphate. This could be due to several reasons. For example, there might be a pH-change near the surface of the membrane, changing the charge of the phosphate anion. Additionally, the PAH-Gu membrane did show an increase in overall anion flux compared to the bare membrane. These results are promising and warrant further research into phosphate selective receptors in combination with IEMs.

# Contents

<b>1</b>	<b>Introduction</b>	<b>4</b>
1.1	Phosphates and the environment . . . . .	4
1.2	Phosphate recovery and ion-exchange membranes . . . . .	5
1.3	Aim of the work . . . . .	5
1.4	Thesis Outline . . . . .	6
<b>2</b>	<b>Theory</b>	<b>7</b>
2.1	Phosphate species and relevant ions . . . . .	7
2.2	IEM mechanism and applications . . . . .	9
2.3	AEM Modification . . . . .	13
2.3.1	Motivation . . . . .	13
2.3.2	LbL Modification . . . . .	14
2.4	Direct Current Resistance . . . . .	16
2.4.1	IEM System Resistance . . . . .	16
2.4.2	Bulk Solution Resistance . . . . .	18
2.4.3	DBL Resistance and Limiting Current Density . . . . .	19
2.4.4	EDL Resistance . . . . .	22
2.4.5	Membrane Resistance . . . . .	23
2.5	Electrochemical Impedance Spectroscopy . . . . .	23
2.5.1	Motivation . . . . .	23
2.5.2	EIS theory . . . . .	24
2.5.3	IEM System Impedance . . . . .	27
2.5.4	DBL Impedance . . . . .	28
2.5.5	EDL Impedance . . . . .	29
2.5.6	Impedance Simulations . . . . .	29
2.5.7	Electrical Equivalent Circuit . . . . .	31
2.6	Electrodialysis . . . . .	34
<b>3</b>	<b>Materials &amp; Methods</b>	<b>36</b>
3.1	Chemicals . . . . .	36
3.2	Membrane Modification . . . . .	36
3.3	Main Electrodialysis Setup . . . . .	37
3.4	EIS Setup . . . . .	39
3.5	Electrodialysis Setup . . . . .	40

<b>4</b>	<b>Results &amp; Discussion</b>	<b>41</b>
4.1	Asymmetric vs Symmetric modification . . . . .	41
4.2	Electrochemical Impedance Measurements . . . . .	43
4.2.1	Membrane Resistance . . . . .	43
4.2.2	DBL Impedance . . . . .	45
4.2.3	EDL Impedance . . . . .	46
4.3	Electrodialysis . . . . .	48
<b>5</b>	<b>Conclusion</b>	<b>53</b>
5.1	Asymmetric vs Symmetric LbL . . . . .	53
5.2	Electrochemical Impedance Measurements . . . . .	53
5.3	Electrodialysis . . . . .	54
<b>6</b>	<b>Outlook</b>	<b>55</b>
<b>A</b>	<b>Integral with complex arguments</b>	<b>57</b>
<b>B</b>	<b>EIS Raw Data</b>	<b>58</b>
<b>C</b>	<b>Fitting to the EEC</b>	<b>59</b>
<b>D</b>	<b>Linear model fitting to ED data</b>	<b>61</b>
	<b>Nomenclature</b>	<b>62</b>

# *Acknowledgements*

First, I would like to thank everyone at the OMI group of TU Delft for the great atmosphere, nice discussions and for all the help they gave me, in and outside the lab. Of course, I would like to thank Prof. dr. E.J.R. Sudhölter for including me in the group and giving me good advice during the project. Furthermore, I would like to thank Duco Bosma for helping me a lot in the lab with the setup and the fun debates we had.

A big thanks to Dr. Lukasz Poltorak for the great guidance he gave me during my thesis, and also the time he invested to figure out problems with me.

Finally, I would like to thank Laura Paltrinieri, MSc. I have a lot of gratitude for the patience you had with explaining things during the whole project and your constant optimism.

Lastly, a thank you to my parents for their never-ending support and motivation.

# 1. Introduction

## 1.1. Phosphates and the environment

The chemical structure of phosphoric acid can be seen in Figure 1. Phosphates play a pivotal role in all biological systems, as a vital nutrient. Phosphorus itself is never found as a free element in nature, due to its highly reactive properties. Pure white phosphorus will, for example, self-ignite when it comes into contact with oxygen. The historical sources of phosphorus used to be manure and guano. Nowadays over 80% is mined from phosphate rock [8]. About 90% of our use of the element is for the food supply chain, mainly in the form of fertilizers and food additives [51]. The annual demand for this ingredient rises nearly twice as fast as the growth of the human population. The large scale use of phosphorous-based chemicals has led to an increase of phosphate concentration in our wastewater [33]. Since this is a great nutrient, the elevated phosphate concentration in lakes and rivers, leads to a process called eutrophication. A high availability of phosphorus promotes the growth of simple algae and plankton. This leads to a shortage of oxygen in the water. The largest negative impact can be traced to two main sources:

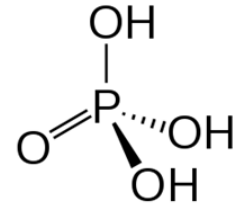


Figure 1.1: Phosphoric acid molecule

1. Decrease in the biodiversity, since some species will die out.
2. Toxicity of the water might rise due to the stimulated growth of certain algae blooms.

For this reason, a lot of countries have placed strict rules on the phosphate concentration in wastewater. The Dutch government has set an upper limit of 0.15 mg/L for the municipal ground water [40].

On the other hand, the phosphate reserves are getting depleted due to a high rate of consumption, mainly for agriculture, but also in the cosmetic sector. Estimations are that in the next 20-40 years our use of them must be “drastically reduced or we will begin to starve” [21].

The need for a reduction of phosphate in wastewater streams and the depletion of primary resources, recalled a potential new market in the sustainable recovery of phosphate directly from wastewater. The Swiss government is the first in the world to enforce a resource recovery from their wastewater, which includes phosphorus [13].

There is a very high likelihood that other countries will follow since phosphate rock is placed in the top 20 of critical raw materials by the European Union [15].

## 1.2. *Phosphate recovery and ion-exchange membranes*

Different methodologies have already been developed for the recovery of phosphate from wastewater. It is estimated that there are more than 30 different methods for P-recovery, underlining its importance [27]. The methods that are currently applied in sewage treatment plants mostly use a chemical or biological approach. The chemical approach is based on a precipitation reaction in which the sewage water is leached with acid and salts of specific metals [31]. The problem with this method is the high costs and the disposal of the concentrated sludge that is left afterwards. The biological approach uses organisms that accumulate the phosphorous from the wastewater, which is consequently retrieved [56]. The disadvantage of this method also lies in the waste that is produced. The micro-organisms are added to the concentrated sludge that is left behind from the chemical approach. This means that the heavy metals that are present in this sludge will also be in the end-product of the biological approach. Also, the operating conditions are strict and hard to achieve.

Recently, membrane technology was used for the recovery process. For example, there are novel ideas to combine osmosis membranes in the biological approach to get a better accumulation and less unwanted collateral materials [48]. Also, a way to improve the chemical approach has been researched, where ion exchange membranes have been used in conjunction with precipitation processes [58].

## 1.3. *Aim of the work*

In this research, we will focus on using ion exchange membranes (IEM's) as a standalone method for phosphorous recovery. The key idea is to selectively transport phosphate ions across the ion exchange membrane in the presence of competing anions. To reach this goal we need to have a low electrical resistance for the phosphate ions, which means a higher transport rate of phosphate with a constant current regime. To improve selectivity towards phosphate, a commercial anion exchange membrane is modified at the surface with a phosphate-selective receptor, through layer-by-layer (LbL) deposition of functionalized polyelectrolytes. Poly(diallyldimethylammonium chloride) (PDADMAC), poly(allylamine hydrochloride) (PAH), and poly(allylamine hydrochloride)-Guanidinium (PAH-Gu) are used for the polyelectrolyte layers. LbL

modification is done on either one side of the membrane, or on both sides. Membrane transport properties are then characterized with electrochemical impedance spectroscopy (EIS) at different phosphate concentrations. The effect of the type of modification and salt concentration is compared in terms of membrane resistance. Finally, the selectivity among phosphate and sulphate anions of modified and unmodified AEM are tested in an electro dialysis set-up. The research questions can be summarized as follows:

1. Is there a difference between symmetric and asymmetric LbL modification on the membranes electrical properties?
2. To which extent does the type of polyelectrolyte affect the membrane resistance towards phosphate for a certain concentration range?
3. Is there an improved discriminatory function of the modified AEM on the transport of phosphate with respect to sulphate?

## 1.4. *Thesis Outline*

This thesis can be seen as composed out of two parts:

- The characterization of a membrane through EIS.
- The permselectivity measurements through electro dialysis.

Both parts share a common background. In Sections 2.1-2.3 we will explain this first. Then we will move on to the theory behind each of the two different techniques. In Chapter 3 we will start again from the shared background, i.e. the chemicals and the electro dialysis machine setup. Afterwards, we continue with the methods behind EIS and the permselectivity measurements. Chapter 4 contains the results and discussion of all the measurements and in Chapter 5 we will give the conclusions that we can draw from our investigation. We conclude with an outlook on future work in Chapter 6.

## 2. Theory

### 2.1. Phosphate species and relevant ions

Returning to the previously mentioned phosphoric acid, it is known that this molecule can donate a proton ( $\text{H}^+$ ) which would leave it negatively charged. When the deprotonation occurs we are left with a negatively charged ion in the form of  $\text{H}_2\text{PO}_4^-$ , called the dihydrogen phosphate anion. This donation can happen again and the resulting molecule has a negative charge of 2,  $\text{HPO}_4^{2-}$ , the hydrogen phosphate anion. When it loses its last proton, we have just the phosphorus atom with 3 negatively charged and 1 neutral O atom, the phosphate anion. These 4 different states happen gradually at 3 different pH-values. The following equilibrium reactions summarize this speciation:



where  $\text{p}K_{\text{a}}$  is the logarithmic acid dissociation constant. This is the pH value at which the dissociation is at an equilibrium. Based on these equations we can easily get the fraction of each species in our solution,  $f$ . We first introduce a variable D, based on the molar concentration of hydrogen ions,  $[\text{H}^+]$ :

$$D = [\text{H}^+]^3 + K_{\text{a}1}[\text{H}^+]^2 + K_{\text{a}1}K_{\text{a}2}[\text{H}^+] + K_{\text{a}1}K_{\text{a}2}K_{\text{a}3} \quad (2.4)$$

Here  $K_{\text{a}}$  are the non-logarithmic acid dissociation constants. The following equations show the method to obtain the species fraction [2]:

$$f_{\text{PO}_4^{3-}} = \frac{[\text{H}^+]^3}{D} \quad (2.5)$$

$$f_{\text{HPO}_4^{2-}} = K_{\text{a}1} \frac{[\text{H}^+]^2}{D} \quad (2.6)$$

$$f_{\text{H}_2\text{PO}_4^-} = K_{\text{a}1}K_{\text{a}2} \frac{[\text{H}^+]}{D} \quad (2.7)$$

$$f_{\text{H}_3\text{PO}_4} = K_{\text{a}1}K_{\text{a}2}K_{\text{a}3} \frac{1}{D} \quad (2.8)$$

To get a clear overview of the fraction of each different species at a given pH level (pH is approximately  $-\log_{10}[\text{H}^+]$ ), we can refer to Figure 2.1.

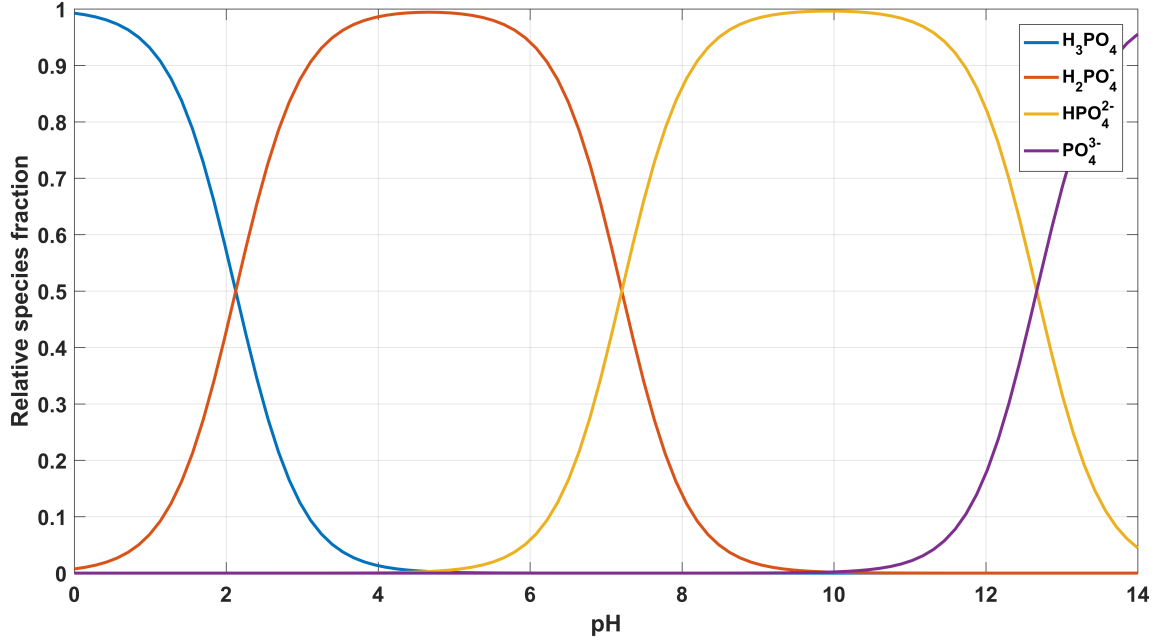


Figure 2.1: The speciation diagram for phosphoric acid

In this research, we will use multiple salts beside phosphates. The diffusion coefficients,  $D$ , and Stokes radii,  $r$ , of the corresponding ions can be found in Table 2.1. The Stokes radii have been calculated based on the diffusion coefficients with the following equation:

$$r = \frac{k_{\text{B}}T}{6\pi\mu D} \quad (2.9)$$

where  $k_{\text{B}}$  is the Boltzmann constant,  $\mu$  the viscosity of the solvent and  $T$  the absolute temperature [2]. The Stokes radius of an ion is the radius of a hard sphere that diffuses at the same speed as the ion in a solution. The diffusion coefficients are taken from [34].

Table 2.1: Properties of the different ions of interest to this research at infinite dilution in water at 25 °C.

Ion	Type	Diffusion coefficient ( $10^{-9} \text{ m}^2 \text{ s}$ )	Stokes radius ( $\text{\AA}$ )
$\text{H}_2\text{PO}_4^-$	Anion	0.96	2.6
$\text{HPO}_4^{2-}$	Anion	0.76	3.2
$\text{SO}_4^{2-}$	Anion	1.06	2.3
$\text{Cl}^-$	Anion	2.03	1.2
$\text{OH}^-$	Anion	5.28	0.46
$\text{Na}^+$	Cation	1.33	1.8
$\text{H}^+$	Cation	9.31	0.26

## 2.2. *IEM mechanism and applications*

Ion-exchange membranes have been investigated and used for over six decades [26]. They have attracted a great deal of attention from the scientific community due to their wide range of applications such as in fuel cells [38], the desalination of seawater [52] and even for renewable energy harvesting in the form of reverse electrodialysis [35]. In this research though, we will be studying their transport properties related to phosphate removal through forward electrodialysis.

An ion-exchange membrane is defined as a layer of material that separates two solution phases. The membrane contains fixed-charged groups and is partially or fully permeable to one or multiple dissolved ion types. IEMs can be classified based on a wide range of inherent properties, such as the polymer material of which it is comprised (hydrocarbon, inorganic etc. [53]) or the microstructure of the polymer framework (homogenous or heterogeneous). The most important categorization however is established by the function of the fixed-charge groups [52]. The two most common types in this regard are:

- Anion exchange membranes (AEM)
  - Contains positively charged groups fixed to the polymer matrix.
  - The membrane permeates only (ideally) anions (negatively charged ions).
- Cation exchange membranes (CEM)
  - Contains negatively charged groups fixed to the polymer matrix.

- The membrane permeates only (ideally) cations (positively charged ions).

A schematic illustration of an anion exchange membrane is shown in Figure 2.2. In the case of an AEM, the mobile anions are able to permeate through the membrane, while the cations are excluded from this transport. The force used to facilitate this transport is the result of a potential difference over the membrane which can be either chemical and/or electrical. The reason for this behavior is that the anions interact with the positive fixed charges in the membrane's framework. Anions are in this case known as the counter-ions and the cations as the co-ions, due to their charge countering or coinciding with the fixed-charged groups of the membrane. These fixed charges in the membrane are usually permanently charged functionalities attached to the polymeric building blocks.

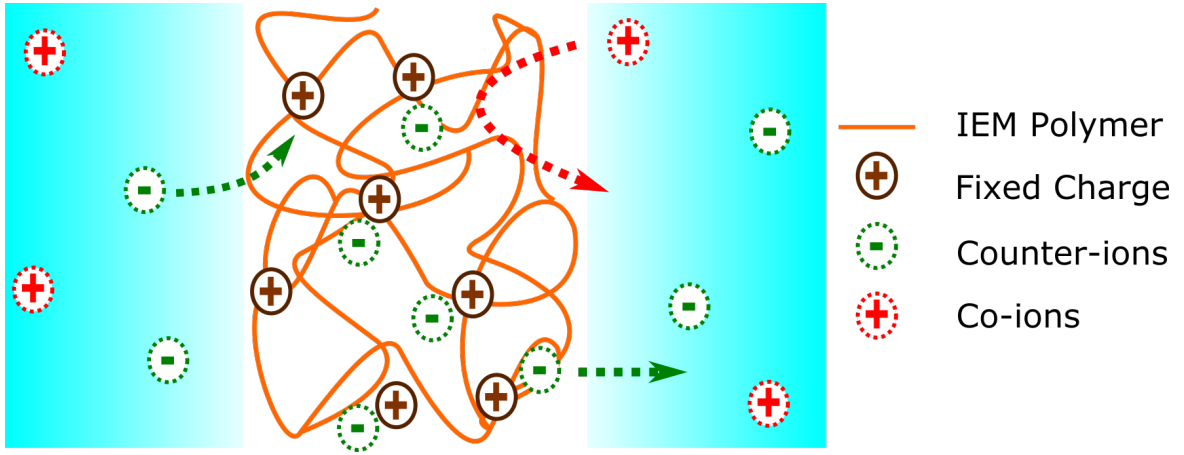


Figure 2.2: Overview of an anion exchange membrane system

It can be seen in the figure that the negative ions are transported from left to right, while the positive ions are completely excluded from the membrane. This discriminatory function is the most fundamental characteristic of an IEM. It can be understood through the Donnan equilibrium theory [12], which I will quickly summarize here, following Tanaka's method [53].

We start from the equation describing the electrochemical potential of component  $i$  in a system:

$$\eta_i = \mu_i^0 + RT \ln(a_i) + (P - P_0)V_i + z_i F \phi \quad (2.10)$$

Here  $\mu_i^0$  is the standard chemical potential,  $R$  the gas constant,  $a_i$  the activity,  $P$  the local pressure,  $P^0$  the standard pressure,  $V_i$  the partial molar volume,  $z_i$  the charge number (valence),  $F$  is Faraday's constant and  $\phi$  is the electric potential. The activity

is defined as  $a_i = \gamma_i C_i$ , where  $\gamma_i$  is the activity coefficient and  $C_i$  is the concentration. When we have a cation X and an anion Y dissolved into a solvent W, we get three equations describing the chemical potentials of each component in the solution phase. The Donnan equilibrium state shows that the electrochemical potential of component  $i$  in the solution phase,  $\eta_i$ , is equivalent to that in the membrane phase.

$$\eta_i = \overline{\eta}_i \quad (2.11)$$

We will work out the steps for an anion exchange membrane.

When we apply the Donnan equilibrium to the anions and then subtract the electrochemical potential in the membrane from the one in the solution, we get:

$$\eta_X - \overline{\eta}_X = \mu_i^0 - \overline{\mu}_i^0 + RT \ln\left(\frac{a_X}{\overline{a}_X}\right) - (\overline{P} - P)V_X - z_X F(\overline{\phi} - \phi) = 0 \quad (2.12)$$

where the overline indicates the value of the variable in the membrane. The assumptions and simplifications we now make are:

1. The reference chemical potential in the solution and membrane are equal,  $\mu_i^0 = \overline{\mu}_i^0$ .
2. If there is no concentration difference between both sides of the membrane, the osmotic swelling pressure,  $\overline{P} - P$ , is 0.
  - This also means that the activity of the solvent is the same for the membrane phase as for the solution.
3. We will work with a symmetric electrolyte. This means that if one mole of electrolytes dissociates, we have  $v_X$  moles of cations and  $v_Y$  moles of anions, where  $v_X = v_Y = v$ .

Using the above factors, we get the following expression for the activities of the anions and cations:

$$a_X^{v_X} a_Y^{v_Y} = \overline{a}_X^{v_X} \overline{a}_Y^{v_Y} \quad (2.13)$$

Finally, we will assume that the activity coefficient of cation X,  $\gamma_X$ , and the activity coefficient of anion Y,  $\gamma_Y$ , in the solution and inside the membrane, is 1. In the case of  $\text{NaH}_2\text{PO}_4$  the Donnan equilibrium is shown in equation X:

$$C_{\text{Na}^+} C_{\text{H}_2\text{PO}_4^-} = \overline{C}_{\text{Na}^+} \overline{C}_{\text{H}_2\text{PO}_4^-} \quad (2.14)$$

To maintain electroneutrality in the membrane, the concentration of counter-ions in the membrane ( $\overline{C}_{\text{H}_2\text{PO}_4^-}$ ) is equal to concentration of co-ions in the membrane ( $\overline{C}_{\text{Na}^+}$ ) and the concentration of the fixed-charged groups inside the membrane ( $\overline{C}_F$ ), as follows:

$$\overline{C}_{\text{H}_2\text{PO}_4^-} = \overline{C}_{\text{Na}^+} + \overline{C}_F \quad (2.15)$$

The last two equations can be simplified by  $C = C_{\text{Na}^+} = C_{\text{H}_2\text{PO}_4^-}$  (since this is a symmetric electrolyte). To get the ratio of counter and co-ion concentrations in the membrane as a function of this salt solution concentration, we can combine the last two equations and get:

$$\frac{\overline{C_{\text{H}_2\text{PO}_4^-}}}{\overline{C_{\text{Na}^+}}} = \frac{\sqrt{C_F^{-2} + 4C^2 + C_F}}{\sqrt{C_F^{-2} + 4C^2 - C_F}} \quad (2.16)$$

When we take the solution salt concentration as a variable and use a fixed-charge group concentration of 3 M (a typical concentration for IEM's), we get Figure 2.3 that shows us the ratio.

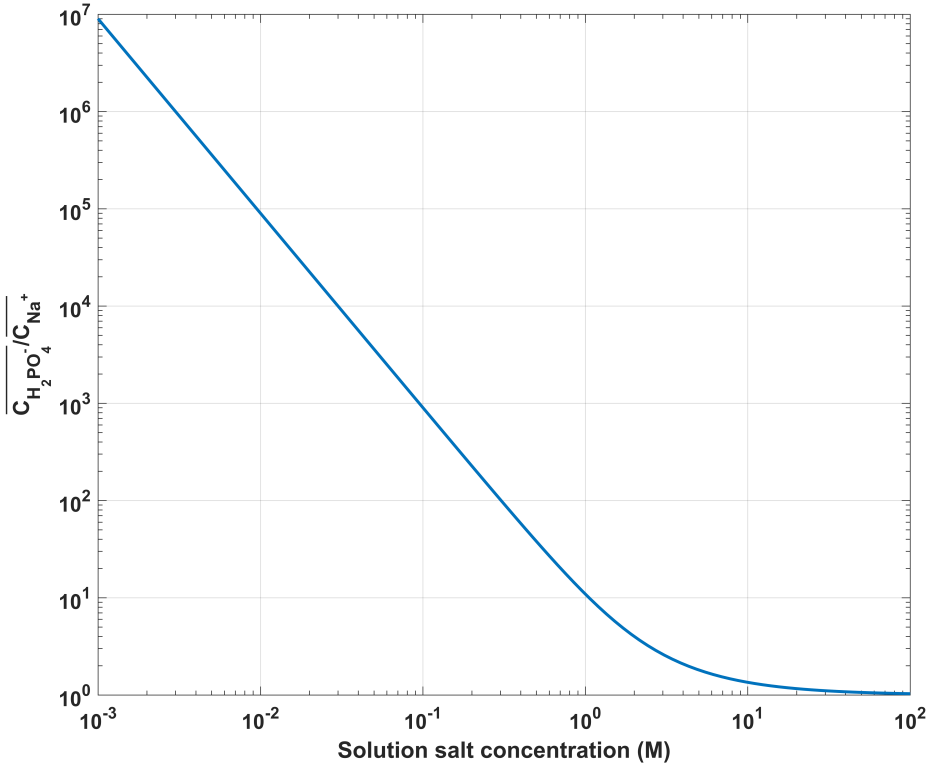


Figure 2.3: Ratio of anion/cation concentration inside the membrane as a function of solution salt concentration.

Another important quantity we can derive from equation 2.12 is the Donnan potential. This is defined as the following electric potential difference:

$$\phi_{Don} = \bar{\phi} - \phi = \frac{RT}{z_X F} \ln\left(\frac{a_X}{\bar{a}_X}\right) \quad (2.17)$$

We will use this later in the report to calculate the electrical resistance between the solution and the membrane.

This gives us a crude, yet meaningful, idea as to why an IEM is selective. It can be seen that for lower concentrations the co-ions are almost completely excluded from the membrane by the fixed-charged groups. When we have an increase in concentration though, this so-called Donnan exclusion, decreases exponentially.

## 2.3. *AEM Modification*

### 2.3.1 Motivation

One of the great disadvantages of commercial anion exchange membranes (AEM) is their poor selectivity. The main goal of our research is to modify an AEM to increase the selectivity for phosphate ions compared to other anions. There are several factors that influence the selectivity of an AEM for phosphate competing with other anions. For example, we need to consider the mobility of the ion of interest. If the diffusion coefficient is low, the transport will be severely limited (values for some relevant ions can be found in Table 2.1). Also, the solution salt concentration, the applied current density, the concentration gradient and a few other minor factors play a role. One of the most important aspects is the interaction between the fixed-charged groups of the membrane and the anions that are transported. This interaction is mainly determined by electrostatic forces and the membrane's chemical-structure properties [6]. Membranes with a high crosslinking density ensure a good selectivity among anions with differences in size. A dense membrane would hinder the diffusion of larger ions through the membrane structure and increase the monovalent permselectivity [1]. Phosphate is a bigger anion compared to others (see Table 2.1). Therefore, tuning the membrane crosslinking degree will not guarantee a higher phosphate selectivity.

A different strategy to increase the phosphate selectivity, is the introduction of specific binding groups into the membrane framework. In the literature this was done by deposition of a thin negatively charged layer on top of a commercial AEM [54] [22]. By applying this polymer layer, the selectivity towards monovalent ions increases. To further improve this method, we employ in this research a layer-by-layer (LbL) assembly of multiple polyelectrolyte layers. First, a bare AEM was exposed to a solution of an anionic polyelectrolyte (PSS), resulting in the formation of a negatively charged monolayer. Subsequently, rinsing off and applying in the same manner a cationic polyelectrolyte, creates a bilayer which terminated with a positive charge. We can form multiple layers of polyelectrolytes by repeating this process [10].

The LbL approach (the end result is also known as a polyelectrolyte multilayer, PEM) has emerged as a facile and precise method to tailor membrane surface properties [25]. A recent application of this method on a CEM with up to 11 bilayers, showed a significant improvement in selectivity for monovalent ions [1]. In this research, we will employ two different methods to modify the membrane. We will modify a bare AEM, a Fuji-AEM-80045, by applying the LbL method to either one side or both sides of the membrane. An overview of the final result can be seen in Figure 2.4. Modification on one-side only yields an asymmetric LbL. When the method is applied to both sides we will call it the symmetric LbL.

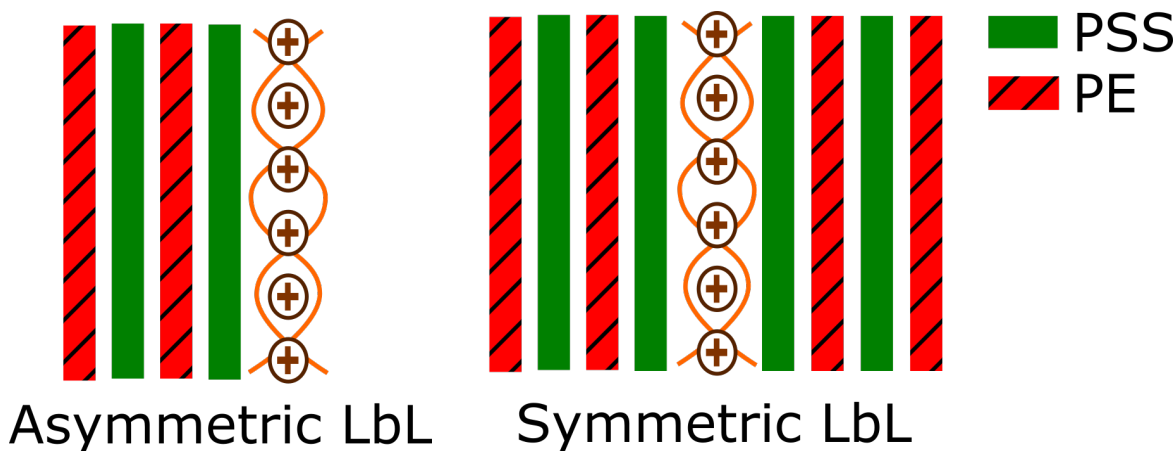


Figure 2.4: Layer by layer modification of an AEM by the asymmetric and symmetric approach. The green layers are PSS and the red layers one of three different polycations.

### 2.3.2 LbL Modification

The first layer will have to be negatively charged in order to have strong electrostatic interactions with the AEM. We used polystyrene sulfate (PSS) for this role. We chose PSS because it can be classified as a strong PE. This means that for almost the whole pH-range it will stay dissociated in water.

The subsequent polycationic layer is expected to modify the transport behavior of phosphate anions. The process behind this mechanism, will be further explained in section 2.4.5. We choose three different polycations for this purpose: Poly(diallyldimethylammonium chloride) (PDADMAC), poly(allylamine hydrochloride) (PAH), and poly(allylamine hydrochloride)-Guanidinium (PAH-Gu). Their chemical structures can be seen in Figure 2.5. An overview of their most important chemical properties is found in Table 2.2. A motivation for this selection will now follow.

We chose PDADMAC, a quaternary ammonium salt, because it has a permanent positive charge in solution. It also resembles the membrane's fixed-charged groups. The bare Fuji membrane we employ in this research, has charged functionalities in the form of quaternary ammonium cation groups. The precise description of these groups, as well as the preparation of the membrane and materials used, are not given because it falls under company-sensitive information.

Recent research showed that PAH-Gu has a high affinity for phosphate with respect to other anions [5]. This characteristic makes it a promising candidate for modifying the membrane in such a way that the selectivity for phosphate increases. The interaction between Guanidinium and phosphate can be seen in Figure 2.6. A ratio of 20:1 is used for the modified PAH-Gu membranes. This means that in Figure 2.5,  $x=1$  and  $y=20$  for the structure of PAH-Gu.

The bare PAH was chosen as a reference for the modified PAH-Gu. This was done to get a better idea of how the Guanidinium affected the ion transport.

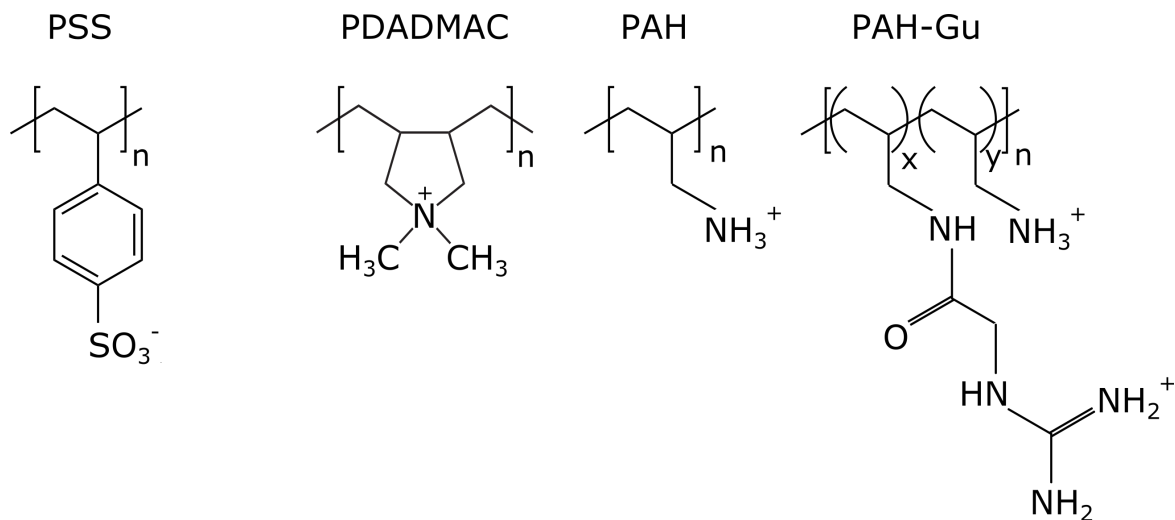


Figure 2.5: Chemical structure of the polyelectrolytes used for LbL modification

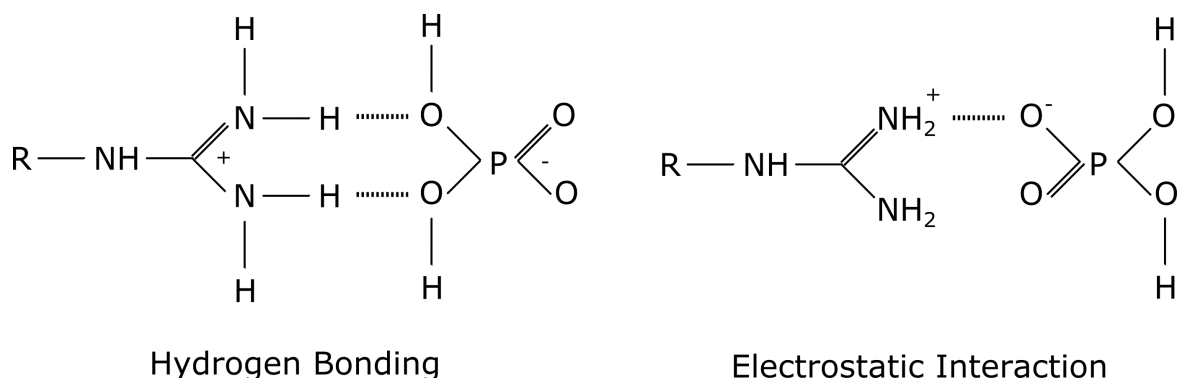


Figure 2.6: The interaction between PAH-Gu and a dihydrogen phosphate anion [30].

Table 2.2: Properties of the polyelectrolytes used for LbL modification

Short Name	Full Name	Fixed Charge	$pK_a$
PSS	Poly(sodium 4-styrene sulfonate)	-	$\sim 1$ [32]
PDADMAC	Poly(diallyldimethylammonium chloride)	+	Permanent positive charge
PAH	Poly(allylamine hydrochloride)	+	$\sim 8.5$ [5]
PAH-Gu	Poly(allylamine hydrochloride)-Guanidinium	+	$\sim 13$ [5]

## 2.4. Direct Current Resistance

### 2.4.1 IEM System Resistance

Transport across an IEM requires a driving force to act on the components of the system [44]. In this research, we will focus on applying an electric potential difference across the membrane that leads to electro dialysis. This is one of the most common applications of IEMs. It is used, for example, to desalinate water on large scale [53] and to a lesser extent it is also used for wastewater treatment. We will use electro dialysis for removal of phosphate anions. In Figure 2.2 the counter-ions are forced to move from left to right under the influence of the applied electric field. The cations will move from right to left, but will be inhibited by the selective membrane.

When we force a current through a wire, the charge carriers, electrons, face a resistance which can be related to the potential by Ohm's law (with a few exceptions, e.g. superconductivity). If we look at an IEM system, the charge carriers are the ions in the solution, and just as their counterparts in the wire, they too face a resistance when they conduct the electric current. In this situation though, the cause of the resistance is a bit more complicated. The resistance of an electric current flow across the electro dialysis cell can be dissected into multiple contributions. An overview of the different components that create electrical resistance, besides the IEM itself, can be seen in Figure 2.7. We will now give a mathematical description which illustrates the transport of ions in each of the separate elements. First we will derive the equations for the application of a direct current (DC) flow. This is done in order to get a comprehensive view on the method that will be deployed to characterize the membranes.

The following derivations are from literature [50] [43] [11]. All literature presumes a case study of a CEM however. For this reason the equations have been heavily modified in this thesis to accommodate the AEM under investigation.

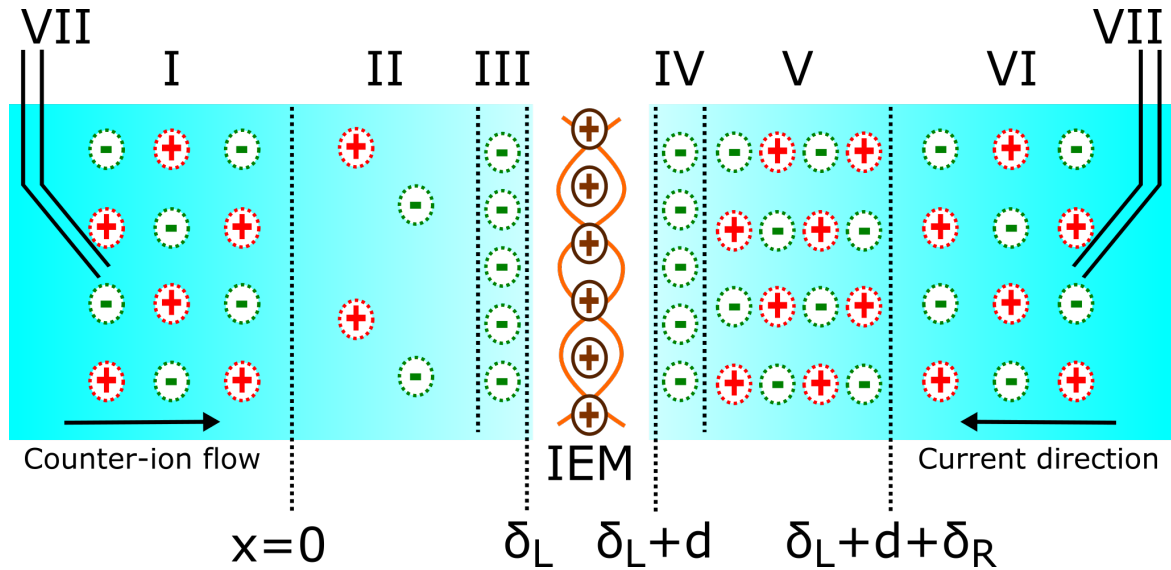


Figure 2.7: The different layers that are formed near the surface of an IEM (width  $d$ ) during transport of ions. I and VI are the bulk solutions. II and V are the diffusive boundary layers (DBL, widths  $\delta_L$  and  $\delta_R$ ). III and IV are the electrical double layers (EDL, pictured without length). VII are Luggin capillaries for potential difference measurements.

## 2.4.2 Bulk Solution Resistance

Before the ions reach the IEM they have to carry the current density that we apply,  $I$ , through the bulk salt solutions. These are indicated by I and VI in Figure 2.7. The ability of an electrolyte solution to conduct electricity is called conductance. Depending on multiple variables such as the dissolved salt type and concentration, the conductivity can be calculated or measured in a fairly straightforward manner. Roughly speaking, if the ion in question has a higher diffusion coefficient, it will be able to carry a current more effectively. In the case of monosodium phosphate (MSP,  $\text{NaH}_2\text{PO}_4$ ) the ions in solution are  $\text{Na}^+$  and  $\text{H}_2\text{PO}_4^-$  (for the specific pH range), and they have equal concentrations. As we can see in table 2.1 the diffusion coefficients,  $D$ , of these two charge carriers are comparable. To get a good picture of the motion of ions in a solution, we start from the Nernst-Planck (NP) equation [9], which describes the flux,  $j$ , of ion  $i$ . It is composed of three different factors:

1. A concentration gradient,  $\nabla c_i$ . This leads to diffusion of the particles.
2. An electromagnetic field,  $\mathbf{E} = \nabla\phi + \frac{\partial\mathbf{A}}{\partial t}$ . This leads to electromigration.
3. The fluid motion,  $\mathbf{v}_f$ . This leads to convection.

The NP equation is:

$$\mathbf{j}_i = - \left[ D_i \nabla c_i - \mathbf{v}_f c_i + \frac{D_i z_i e}{k_B T} c_i (\nabla\phi + \frac{\partial\mathbf{A}}{\partial t}) \right] \quad (2.18)$$

Here  $\mathbf{v}_f$  is the fluid velocity,  $z_i$  is the charge number of ion  $i$  and  $\mathbf{A}$  is the magnetic potential. We make a few simplifications and assumptions:

1. We work in a side-view reference frame. So we have one dimension where the length scale is given in Figure 2.7.
2. To simplify the calculations we define the electric field as  $E = \frac{e}{k_B T} \nabla\phi \stackrel{1-D}{=} \frac{F}{RT} \frac{\partial\phi}{\partial x}$ .
3. The velocity  $\mathbf{v}_f$  is 0, since we can assume no net mass transfer of the fluid through the membrane.
  - This assumption holds for the rest of our research and will be applied to **all** other equations in this thesis.
4. We assume static electromagnetic conditions. In this case we can drop the vector potential term,  $\mathbf{A}$ .

- This assumption also holds for the rest of the thesis.

5. If the solution is well mixed, the concentration gradient  $\nabla c_i$  can also be set to 0.

- This assumption holds for the bulk solution but in general is not applicable to other parts of the IEM system. We will change this accordingly for these regions.

These simplifications lead to a much shorter equation for the flux of ion  $i$  in our bulk solution:

$$j_i = D_i z_i c_i E \quad (2.19)$$

The total Faradaic current density is the sum of these fluxes for the ions:

$$I = F \sum z_i j_i \quad (2.20)$$

$$= F(D_1 z_1^2 c_1 + D_2 z_2^2 c_2) E \quad (2.21)$$

where subscript 1 indicates the anion and 2 the cation. Equation 2.20 is called the current flow condition. In the case of MSP we have  $z_1 = -1$  and  $z_2 = 1$ . Since there is electroneutrality we also have  $c_1 = c_2 = c$ . This gives us an expression for the electric field in the electrolyte solution:

$$E = \frac{I}{Fc(D_1 z_1^2 + D_2 z_2^2)} \quad (2.22)$$

When we combine this with the simplified equation for the flux, we are left with:

$$j_1 = \frac{I}{F z_1} t_1 \quad \text{where} \quad t_1 = \frac{D_1}{D_1 + D_2} \quad (2.23)$$

$$j_2 = \frac{I}{F z_2} t_2 \quad \text{where} \quad t_2 = \frac{D_2}{D_1 + D_2} \quad (2.24)$$

$t_1$  and  $t_2$  are called the transference numbers and indicate the fraction of the current transported by each specific anion. This means that if we apply a current through a solution of monosodium phosphate, about 42% of the current is transported by phosphate anions and the other 58% by the sodium cations. The electrical resistance of the bulk solution layer will be denoted by  $R_s$ .

### 2.4.3 DBL Resistance and Limiting Current Density

As the ions come closer to the IEM, they encounter a region called the diffuse boundary layer (DBL) or stagnant diffusion layer (SDL). These are indicated by II and V in

Figure 2.7. This region is formed due to a depletion (or over-saturation on the receiving side) of charge carriers [50]. This shortage is caused by the high transport number of counter-ions in the membrane. In the membrane a large amount (ideally all) of the current is carried by the counter-ions. We can quantify this as the fraction of the current carried by the counter-ions through the solution/membrane interface. This is called the effective transport number of the counter ions,  $T_1$ . On the other hand, as we saw in Section 2.4.2, about half of the current is carried by the anion in the bulk solution,  $t_1$ . This discrepancy leads to a lower concentration of counter-ions in the DBL region. To maintain electroneutrality, the concentration of both ions drops [28]. This layer is of major importance for electrodialysis since it can induce a significant electrical resistance. Especially in reverse electrodialysis there is a lot research underway in minimizing this resistance to gain a higher power output [55].

The DBL can be quite wide and is usually on the order of hundreds of micrometers [7]. In our reference figure they have a width of  $\delta_L$  and  $\delta_R$  for the left and right side, respectively. Since it is still relatively far from the IEM itself, this layer mostly depends on factors not relating to the membrane (we assume no homogeneities on the membrane surface). A major impact on the formation of this layer is the speed at which the bulk solution is stirred or flowed next to the membrane [46]. We see in Figure 2.8 that the depleted DBL (left side) contains a lower concentration of ions than the enriched layer on the other side of the membrane.

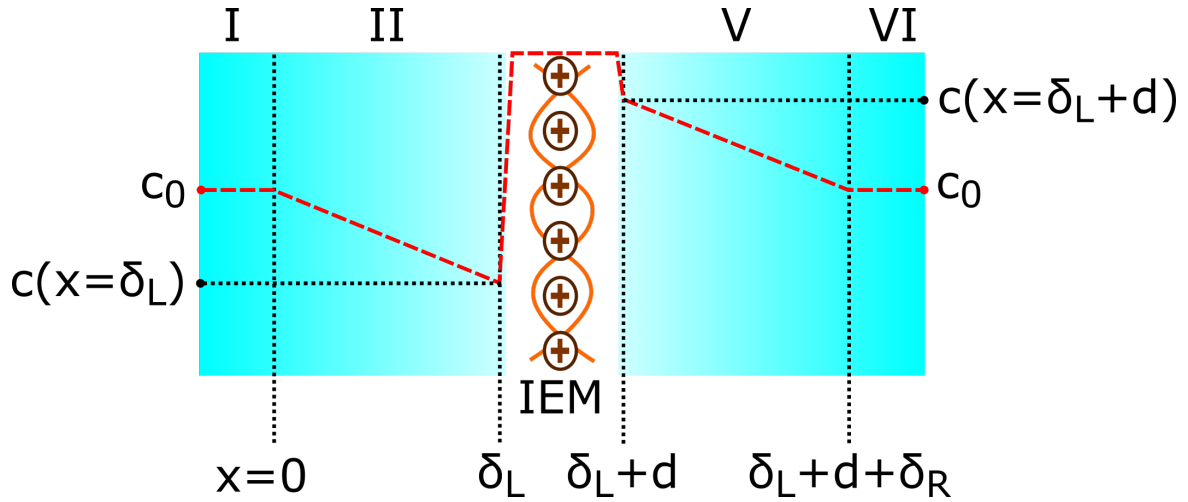


Figure 2.8: The ion concentration profile near an IEM in red striped lines. I and VI are the bulk solutions. II and V are the diffusive boundary layers (widths  $\delta_L$  and  $\delta_R$ ).

This means that if we apply a large enough current we can completely deplete this

layer. When this occurs, we can increase the potential, but the current density will not rise anymore. This is called the Limiting Current Density (LCD) of the membrane. It was already observed in 1956 that the LCD can be calculated by using the following equation, known today as Peers equation [47]:

$$I_{lim}^k = \frac{FD_s c_0}{\delta_k(T_1 - t_1)} \quad (2.25)$$

where  $c_0$  is the bulk solution's ion concentration,  $k$  denotes the side of the membrane ( $L$  for left,  $R$  for right) and  $T_1$  is the effective transport number. Furthermore,  $D_s$  is the salt diffusion coefficient [43]. It is defined as:

$$D_s = \frac{2D_1D_2}{D_1 + D_2} \quad (2.26)$$

It is important to note that the derivations made are for the left side of the membrane,  $k = L$ . We will drop the subscript for readability and will only give the end-result for the right side. Also, to make calculations tidier we introduce the following variable:

$$\beta = \frac{I}{I_{lim}} \quad (2.27)$$

which gives the fraction of the applied current density compared to the LCD.

To calculate the resistance of the DBL, we can use the NP equation again. Only this time the assumption that there is no concentration gradient, does not hold. We start with the following equation for the flux of an ion  $i$  in the DBL region:

$$j_i = -D_i \left[ \frac{dc}{dx} + z_i c_i E \right] \quad (2.28)$$

Now we use the current flow condition in the same manner as we did for the bulk solution resistance. This gives us the following equation for the electric field in the DBL:

$$E = (2t_1 - 1) \frac{dc}{cdx} + \frac{I}{(D_1 + D_2)cF} \quad (2.29)$$

Continuing the same line of reasoning as in Section 2.4.2, we get the flux of each ion species:

$$j_1 = -D_s \frac{dc}{dx} + \frac{I}{Fz_1} t_1 \quad (2.30)$$

$$j_2 = -D_s \frac{dc}{dx} + \frac{I}{Fz_2} t_2 \quad (2.31)$$

To find the resistance, we need to apply boundary conditions (BCs). The first BC is for the concentration at the left side of the DBL. The second set is for the continuity of flux at the DBL/EDL interface:

$$c(x = 0) = c_0 \quad (2.32)$$

$$j_1(x = \delta_L) = -\frac{IT_1}{F} \quad \text{and} \quad j_2(x = \delta_L) = \frac{I(1 - T_1)}{F} \quad (2.33)$$

We set  $T_1 = 1$ . This implies that there is no flux of co-ions at the membrane surface. In other words, all the current is carried by the counter-ions and we have a perfect membrane as a simplification. With these BC's we can get the ion concentration on the left side of the membrane:

$$c(x) = c_0 \left[ 1 - \beta \frac{x}{\delta_L} \right] \quad (2.34)$$

This leads to the concentration curves we can see in Figure 2.8. Since we know that the electric field can be seen as the negative gradient of the electric potential, we now have a way to calculate the potential drop over the left DBL:

$$\frac{\partial \phi}{\partial x} = -\frac{RT}{F} E \quad (2.35)$$

$$\phi_{DBL} = -\frac{RT}{F} \int_0^{\delta_L} E dx = -\frac{RT}{F} \ln(1 - \beta) \quad (2.36)$$

We can use the same steps to get the potential drop on the right side of the membrane:

$$\phi_{DBL}^R = \frac{RT}{F} \ln(1 + \beta) \quad (2.37)$$

With the above electric potential differences, we can use the well known relations between potential, current and resistance to get the resistance of the DBL. We will denote it as  $R_{DBL}$ .

#### 2.4.4 EDL Resistance

After the charge carriers have passed the DBL they are suddenly strongly attracted to the surface of the charged IEM. This high concentration of counter ions is there to screen the surface charge [3]. This layer is very thin, on the order of the Debye length, which for an electrolyte solution is given by:

$$L_D = \sqrt{\frac{\epsilon \epsilon_0 RT}{2cF^2}} \quad (2.38)$$

where  $\epsilon$  is the dielectric constant of the medium,  $\epsilon_0$  the permittivity of free space and  $c$  the concentration of the electrolyte.  $L_D$  gives a measure to the distance of the electrostatic fields of charge carriers in a solution. For the salt solutions we use, this length is around a nanometer. The EDL is the only part of the IEM system that is not electroneutral.

To get the resistance of this layer, we turn to the Donnan potential, introduced earlier in Equation 2.17. By applying this equilibrium theory, we get the potential drop over the almost infinitesimal EDL:

$$\phi_{EDL} = -\frac{RT}{F} \ln \left( \frac{c(x = \delta_L)}{c_M} \right) \quad (2.39)$$

where  $c_M$  is the concentration of anions in the membrane. For the right side of the membrane the potential drop is defined as:

$$\phi_{EDL}^R = -\frac{RT}{F} \ln \left( \frac{c_M}{c(x = \delta_R)} \right) \quad (2.40)$$

Just as with the DBL, we can find the resistance of this layer, denoted by  $R_{EDL}$ , through this potential drop.

## 2.4.5 Membrane Resistance

Finally, the most dominant resistance comes from the IEM. The ions face more restricted movement in the membrane than in the solution. The ions that are transported through the membrane constantly weakly interact with the fixed-charged groups. This could be seen in Figure 2.2. Calculating the membrane resistance can be done theoretically. These computations are based on the extended Nernst-Planck equation for the convection velocity,  $\kappa$ . Based on this velocity we can calculate the specific electric conductivity [53]. Unfortunately, most of the parameters that are needed to carry out the calculations, are not readily available. For example, the material of the membrane and how it is organized, which can't easily be quantified, play a huge role on the resistance. For this reason, an objective of this study is to find the membrane resistance through experimental methods. The membrane resistance will be denoted by  $R_m$ .

## 2.5. *Electrochemical Impedance Spectroscopy*

### 2.5.1 Motivation

Since we modify the membrane we would like to know how our applied layers are affecting the transport of ions through the IEM system. We can simply apply a direct

current (DC) and measure the potential drop over the membrane to determine the entire system resistance, which includes all contributions. This is the most convenient method to get the membrane resistance. An experiment done in this manner will yield current-voltage curves that contain a lot of information on the transport properties of the system. This was done on a large scale in older research [36]. It relies on Ohm's law to describe the resistance:

$$R_{s+DBL+EDL+m} = \frac{U}{I} \quad (2.41)$$

where  $R_{s+DBL+EDL+m}$  is the total resistance of the entire system including all its layers. By simply subtracting the resistance of the bulk solution, we can get the resistance of the membrane, including its DB and ED layer. To get a clearer perspective on the individual resistance components of each layer and get a precise value of the variable that we are interested in, we turn our attention to Electrochemical Impedance Spectroscopy (EIS) measurements.

### 2.5.2 EIS theory

EIS is a technique that has been applied in many different types of research and development [4]. It can be used to investigate the processes behind chemical reactions, transport properties and surface of materials [36]. The foundations of this technique date back to 1880, when the "father" of EIS, Oliver Heaviside, derived the framework behind the technique. The power of EIS comes from a few different sources. In this study, we chose this method for the following, most important, reasons:

1. It enables the user to distinguish between all electric parameters of the system. In this case, we can look at the individual contributions of all the components described in Section 2.4.
2. It is non-invasive if very low current/voltage perturbations are applied. Unlike other methods, such as high current density measurements, this technique won't damage the membrane.
3. The theory behind this method is well documented and it is widely deployed in the field of IEMs.

To give an overview of how EIS works, we start with Ohm's law and replace the real-valued resistance term,  $R$ , with the complex-valued **impedance**,  $Z$ :

$$Z = \frac{U}{I} \quad (2.42)$$

Since we are using sinusoidal signals it is easier to represent the current and potential as:

$$I = |I|e^{i\omega t} \quad (2.43)$$

$$U = |U|e^{i(\omega t + \theta)} \quad (2.44)$$

Here  $i$  is the imaginary unit,  $\omega$  is the angular frequency and  $\theta$  is the phase shift of the potential signal. By combining this with equation 2.42, we get:

$$Z = \frac{|U|e^{i(\omega t + \theta)}}{|I|e^{i\omega t}} \quad (2.45)$$

$$= \frac{|U|}{|I|}e^{i\theta} \quad (2.46)$$

$$= |Z|e^{i\theta} = |Z| \cos \theta + i|Z| \sin \theta \quad (2.47)$$

In Equation 2.47 Euler's formula is used. This is known as the polar form of the impedance. The term  $|Z|$  shows the ratio of the potential over current. We can also write this in Cartesian form:

$$Z = \text{Re}\{Z\} + i \text{Im}\{Z\} \quad (2.48)$$

In conclusion, for a given sinusoidal applied signal of frequency  $f$  ( $f = \omega/2\pi$ ) we get an impedance,  $Z$ , that can be seen as the sum of its real and imaginary parts. The real part is the **resistance** while the imaginary contribution is called the **reactance**.

Using a graph with a real and imaginary axis, we can place points recorded at different frequencies. This is called a Nyquist frequency response plot. The procedure for constructing such a plot can be seen in the following figures. In Figure 2.9 we see the alternating current that we apply over our system and the measured potential. We can also see that there is a slight shift between the two variables. By applying equations 2.47 and 2.48 we can construct a point that has a real and imaginary part. This point is then placed on a graph with data from other frequencies. A curve that is characteristic of the system then emerges. This is seen in Figure 2.10.

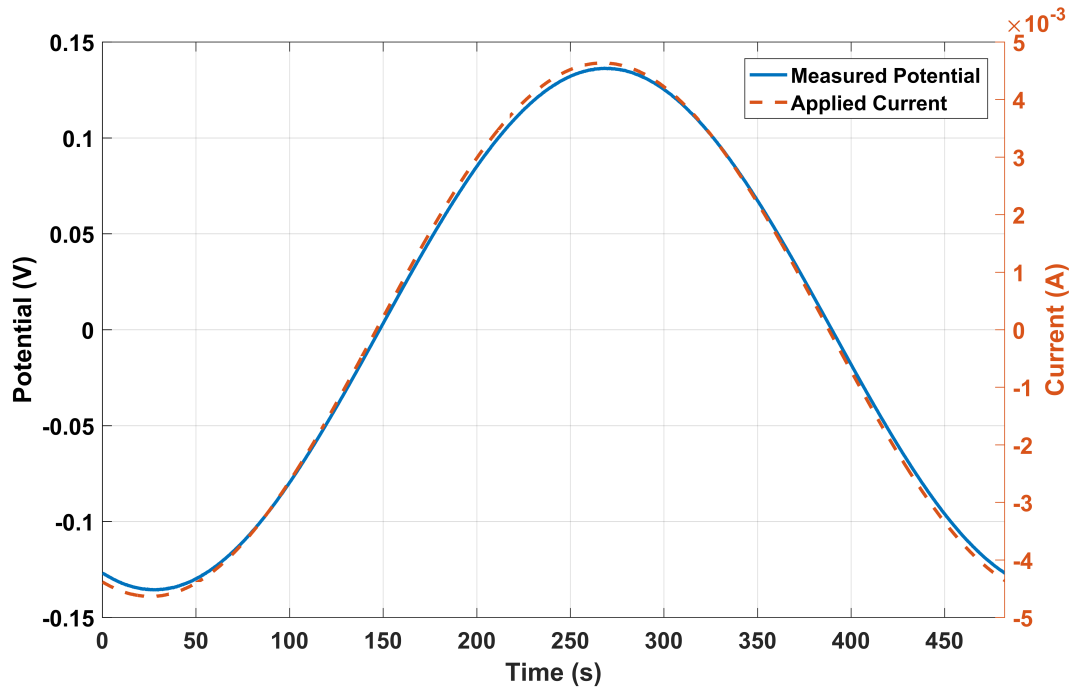


Figure 2.9: The measured potential for a given sinusoidal applied current. The plot was made from impedance spectra data at 2.07 mHz. The phase shift  $\theta$  can be seen by the slight lag of the potential.

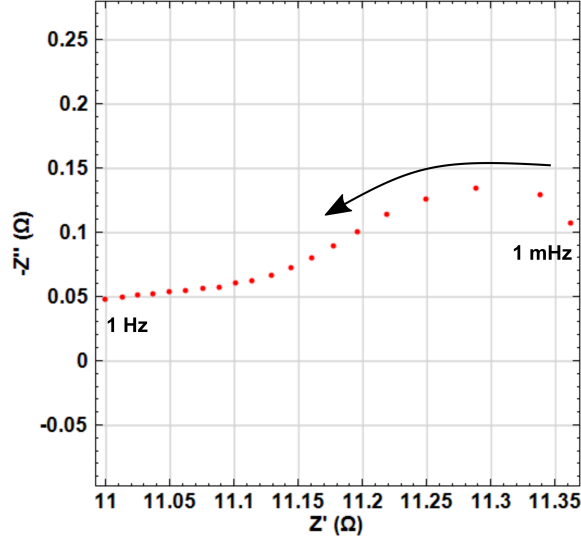


Figure 2.10: The obtained data for multiple frequencies is plotted in a Nyquist plot. Arrow indicates increasing frequency.

### 2.5.3 IEM System Impedance

The previously derived resistances for the IEM system must now be modified to accommodate the alternating, low frequency current that will be applied. The current can be denoted as:

$$I = I_{DC} + I_A e^{i\omega t} \quad (2.49)$$

where  $I_{DC}$  is the steady state, direct current and  $I_A$  is the amplitude of the oscillating current. We now implement the alternating current into concentration and potential oscillations. Both these perturbations follow the same frequency as the AC [41]:

$$c(x, t) = c_{DC}(x) + c_A(x) e^{i\omega t} \quad (2.50)$$

$$\phi(x, t) = \phi_{DC}(x) + \phi_A(x) e^{i\omega t} \quad (2.51)$$

where the subscript  $DC$  indicates the value under a DC condition, and  $A$  is for the amplitude of the variable under the oscillations. We will now apply the above equations to the different resistance components.

The first layer, bulk solution, is the easiest since it has no reactance. In other words  $Z_s = R_s$ .

Furthermore, we will assume that the current transport inside the membrane does not have any reactance either,  $Z_m = R_m$  [50].

## 2.5.4 DBL Impedance

The NP equation introduced in Section 2.4.2 is an extension of Ficks first law of diffusion. It works under the assumption of steady state [9]. Since we are now working with a time dependent factor, we introduce the second Fick equation:

$$\frac{\partial c}{\partial t} = -\frac{\partial j}{\partial x} = D_s \frac{\partial^2 c}{\partial x^2} \quad (2.52)$$

Applying this to Equation 2.50 gives:

$$i\omega c_A = D_s \frac{d^2 c_A}{dx^2} \quad (2.53)$$

We will keep the boundary conditions 2.32 and 2.33, only substituting the steady state concentration with the concentration oscillation  $c_A$ . After a lot of cumbersome calculations, we can find our concentration oscillations.

$$c_A(x, t) = -\frac{I_A c_0}{I_{lim} \alpha} \frac{\sinh(\alpha(x/\delta))}{\cosh(\alpha)} \quad (2.54)$$

where

$$\alpha = \delta \sqrt{\frac{i\omega}{D_s}} \quad (2.55)$$

Applying the above equation for the concentration into 2.29, we find the electric field, and consequently the potential drop.

$$E_A = (2t_1 - 1) \frac{\partial}{\partial x} \left( \frac{c_A}{c_{DC}} \right) + \frac{1}{(D_1 + D_2)F} \left( \frac{I_A}{c_{DC}} - \frac{I c_A}{c_{DC}^2} \right) \quad (2.56)$$

$$\phi_A(x, t) = -\frac{RT}{F} \int_0^\delta E_A dx \quad (2.57)$$

By invoking the modified Ohm's law,  $Z = \phi_A/I_A$ , we finally arrive at the impedance of the left DBL:

$$\begin{aligned} Z_{DBL} = & \frac{RT}{FI_{lim}} \left[ \frac{(1 - 2t_1) \tanh(\alpha)}{(1 - \beta) \alpha} \right. \\ & \left. + \frac{2t_1 t_2 \beta}{(T_1 - t_1) \alpha \cosh(\alpha)} \int_0^\delta \frac{\sinh(\alpha x/\delta) dx}{(1 - \beta x/\delta)^2 \delta} \right] \\ & - \frac{RT}{FI} \frac{2t_1 t_2 \ln(1 - \beta)}{T_1 - t_1} \end{aligned} \quad (2.58)$$

Following the same steps gives us the impedance for the right DBL:

$$\begin{aligned}
Z_{DBL}^R = & \frac{RT}{FI_{lim}^R} \left[ \frac{(1 - 2t_1) \tanh(\alpha^R)}{(1 + \beta^R) \alpha^R} \right. \\
& \left. - \frac{2t_1 t_2 \beta^R}{(T_1 - t_1) \alpha^R \cosh(\alpha^R)} \int_0^{\delta_R} \frac{\sinh(\alpha x / \delta_R) dx}{(1 + \beta^R x / \delta_R)^2 \delta_R} \right] \\
& + \frac{RT}{FI} \frac{2t_1 t_2 \ln(1 + \beta^R)}{T_1 - t_1}
\end{aligned} \tag{2.59}$$

Most software packages can't evaluate an integral of hyperbolic functions with complex arguments. In Appendix A a different expression is given.

### 2.5.5 EDL Impedance

Applying the same procedure for the EDL gives us the following potential drop over the EDL:

$$\phi_A(x, t) = - \frac{I_A}{I_{lim}(1 - \beta)} \frac{\tanh(\alpha)}{\alpha} \tag{2.60}$$

We don't have to integrate over  $x$  since there is no space dependency. The impedance for the left EDL is then given by:

$$Z_{EDL} = \frac{RT}{FI_{lim}} \frac{1}{(1 - \beta)} \frac{\tanh(\alpha)}{\alpha} \tag{2.61}$$

Following the same steps gives us the impedance for the right EDL:

$$Z_{EDL}^R = \frac{RT}{FI_{lim}^R} \frac{1}{(1 + \beta^R)} \frac{\tanh(\alpha^R)}{\alpha^R} \tag{2.62}$$

### 2.5.6 Impedance Simulations

We can combine the potential drop over the DBL and the EDL. To get the impedance of the entire IEM system, we then invoke Equation 2.42. This gives us:

$$Z = R_s + R_m + Z_{DBL}^L + Z_{DBL}^R + Z_{EDL}^L + Z_{EDL}^R \tag{2.63}$$

where  $R_s$  and  $R_m$  are the resistances of the bulk solution (left and right side combined) and the membrane itself.

Theoretically, Equation 2.64 in combination with the explicit formulations, is enough to give a low frequency impedance spectra of an IEM system. Upon close inspection of

the equations we see that there are only 5 variables when we work with a symmetric, monovalent salt. We have the thickness of the DBL on both sides,  $\delta_k$ , the concentration of the salt,  $c_0$ , the applied direct current density,  $I$  (also referred to as  $I_{DC}$  in the calculations for clarity) and the membrane resistance.

With this theoretical model we now have the means to simulate the impedance of our AEM system to quantitatively observe how our impedance spectrum will behave under differing conditions.

It is of importance to know what direct current we need to apply during our EIS measurements. To see the impact of  $I_{DC}$  on the impedance spectra, we will simulate the low frequency impedance with the following fixed variable values:

1.  $\delta_L = \delta_R = 250 \mu\text{m}$ .
2.  $c_0 = 0.5 \text{ M}$ .
3.  $\omega = 2\pi f$  with  $f$  ranging from 1 mHz to 1 Hz.
4.  $R_s = 0 \Omega \text{ cm}^2$  and  $R_m = 30 \Omega \text{ cm}^2$ .
5. Diffusion coefficients as given in Table 2.1 for  $\text{NaH}_2\text{PO}_4$ .

$I_{DC}$  is then chosen as a certain percentage of our  $I_{lim}$ . The result can be seen in Figure 2.11.

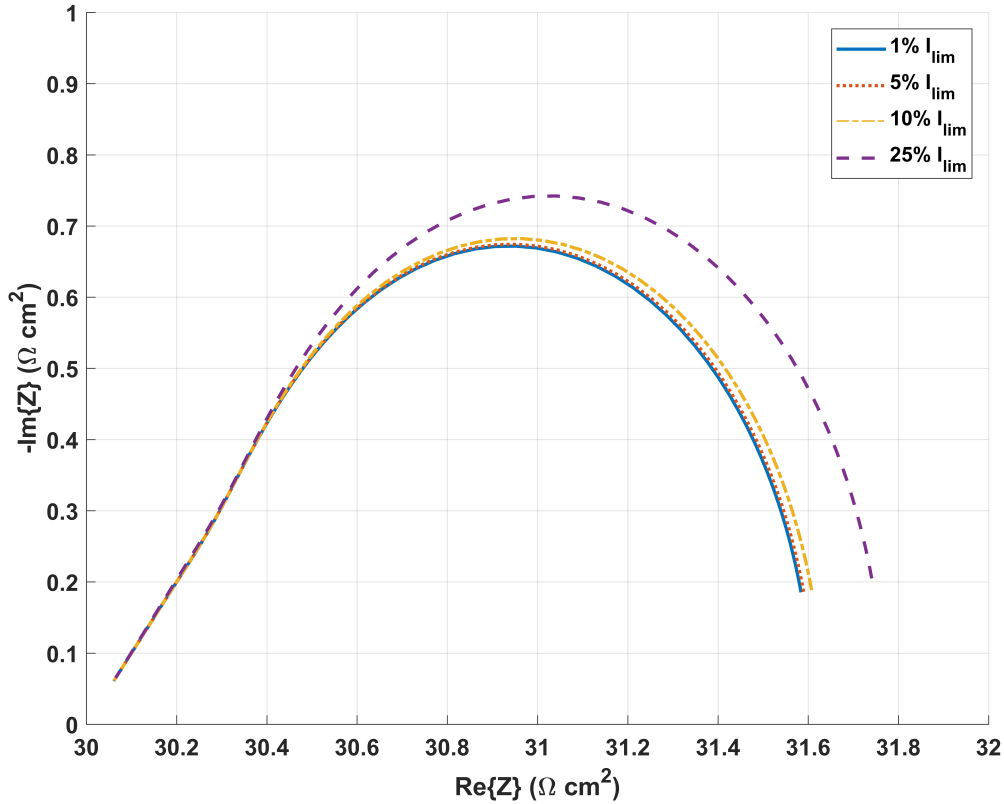


Figure 2.11: Simulation of the low frequency impedance of an anion exchange membrane. The applied direct current is a percentage of the LCD.

It can be noted that there is a convergence for a decrease in the applied direct current density. For this reason we chose to carry out our EIS measurements with an  $I_{DC}$  of  $0 \text{ A cm}^{-2}$ . Additional motivation for this choice will be given in Section 3.4.

### 2.5.7 Electrical Equivalent Circuit

In a review report on EIS by D.D. MacDonald [36], a pioneer in the field, he explains the extraordinary strength of EIS. Unfortunately, the full potential of the method is rarely used because the interpretation of the data requires a strong mathematical skill that is not common among electro-chemists and corrosion scientists. The mathematical background needed to interpret the low frequency impedance of an IEM system, for example, can be seen in the previous sections. Theoretically, the EIS data can be fitted to the complicated equations. Variables such as DBL thickness and membrane

resistance can then be extracted. Unfortunately, this is beyond the scope and reach of this thesis due to the very elaborate mechanisms behind fitting the data. Because of this complexity, the data is usually analyzed, modeled and interpreted via an electrical equivalent circuit (EEC). EECs have been a tool to model the impedance of electrolytic cells for over 40 years and are a classic topic in the electrochemical literature [18]. There are two main viewpoints for using electric circuits.

The first one distributes electrical circuit components in space instead of in a straight linear fashion [41]. The elements lie superimposed on their chemical, real-life equivalents and are controlled by the mathematical equations describing the ion transport, such as the Nernst-Planck and Poisson equations. This is a powerful method and it has shown to be of great use to predict and explain transport phenomena in electrochemical processes [42] [43]. The main disadvantage of this method is the complexity of the models.

The second method uses an EEC with localized parameters. The elements are distributed in a linear order and each different branch of the circuit models a part of the electrochemical system. The strong points of this approach are the ease of use and their effectiveness in explaining experimental data. The downside to this simplicity is the ambiguity that might arise in applying the EEC. For example, an electrochemical system might be modeled by multiple different EECs that all show the same impedance over the given frequency range. For this reason, a great deal of care must be taken to use the correct and most applicable EEC.

The mathematical transport model of a monopolar IEM we introduced in Section 2.5.3, was initially proposed by Sistat et al. [50] In this paper he showed the remarkable agreement between the mathematical description and experiments. Soon, modifications to the model followed. Moya made a lot of contributions, such as modeling ternary solutions with two counterions [42] and an EEC model involving distributed elements [43]. Nikonenko et al. showed the resemblance to an EEC [45] that was composed of 5 different circuits connected in series. In this research, we will use this method to explain our impedance spectroscopy data obtained from measurements on the membranes. We will not use the exact same model as used by Nikonenko, but a slightly modified one. In Figure 2.12 the EEC that will be utilized to model the different components of the IEM system can be seen. This model has been used extensively in other research [1] [11] [17] [46] [57].

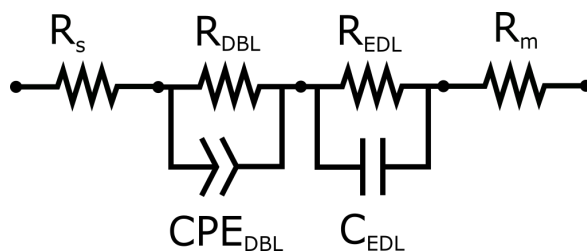


Figure 2.12: The Electrical Equivalent Circuit used in this study to analyze the EIS data.

$R_s$  is the bulk solution resistance, also including the Luggin capillaries and parasitic resistances of the measurement equipment.  $R_m$  is the resistance of the membrane (with LbL layers if they are applied).

$R_{EDL}$  and  $C_{EDL}$  are the resistance and capacitance of the representation of the EDL, respectively. It can be seen from Equations 2.61 and 2.62 that the hyperbolic tangent function plays a huge role in the impedance of the EDL. To model this behaviour a parallel RC circuit was chosen [45], with impedance given by:

$$Z_{EEC,EDL} = \left( \frac{1}{R_{EDL}} + i\omega C_{EDL} \right)^{-1} \quad (2.64)$$

Finally,  $R_{DBL}$  and  $CPE_{DBL}$  are the resistance and constant phase element (CPE) modeling the DBL. The CPE is an element that is used to model the non-homogeneity of the DBL. The impedance is given by:

$$Z_{CPE} = \frac{1}{Q(i\omega)^n} \quad (2.65)$$

A study by Moya [41] compared the EEC model we use with the more complex network model. It was found that the simpler EEC properly models the low-frequency impedance of the IEM system in situations where there is no DC current applied during the EIS measurements.

We only use one branch of the circuit to model the EDL and one branch to model the DBL, whereas there are two of each layer (either membrane side), which may have different properties. This modeling is chosen because even though the EIS method can differentiate between the different layer types, it is hard to separate between the same type due to a large overlap in response to the alternating current.

## 2.6. Electrodialysis

Electrodialysis is a process in which we actively transport ions through the membrane. The external force used to trigger this transport, comes from applying a current through the membrane. The overview of the setup used for this process is shown in Figure 2.13.

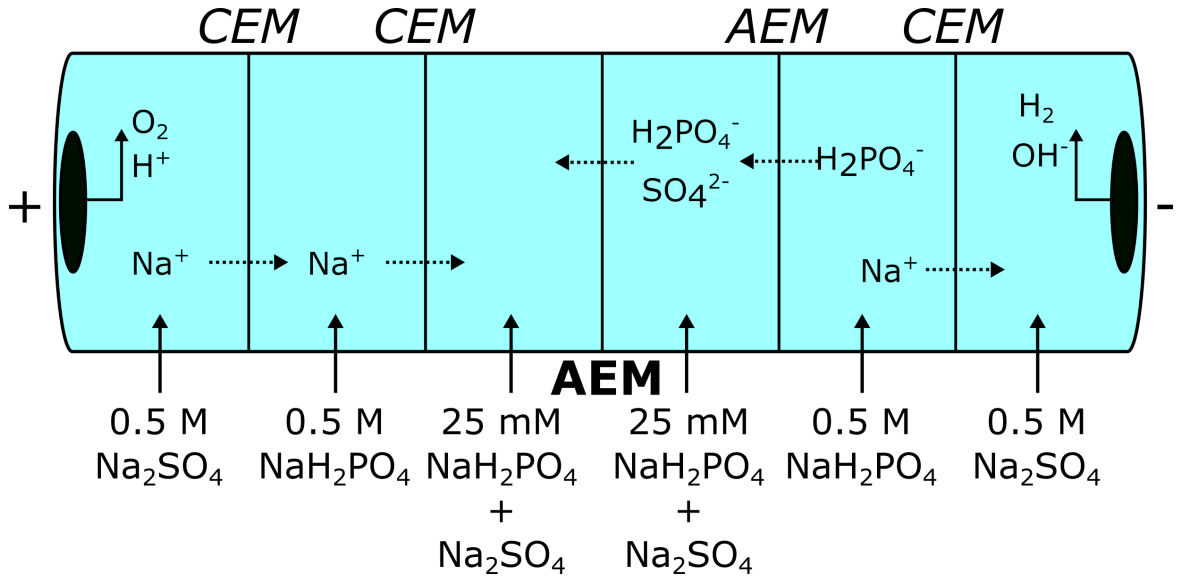


Figure 2.13: Overview of the setup used for electrodialysis.

It can be seen that there are multiple chambers in the complete setup. The purpose of all the chambers will be elaborated in Section 3.3. The most important two cells that we will focus on now are the left and right cells of the boldface AEM in the middle.

The two chambers in the middle are constantly flushed with a mixed solution of phosphate and sulfate (25 mM of each species, explanation for this choice will follow in Section 4.3). This means that there are two types of anions that will, ideally only, travel through the membrane, the divalent sulfate and monovalent phosphate. To quantify the discriminatory function of the membrane we look at the permselectivity for phosphate with respect to sulfate.

First, we need to define the flux for each anion [53]:

$$j_{\text{H}_2\text{PO}_4^-} = \frac{V}{A_m} \frac{dC_{\text{H}_2\text{PO}_4^-}}{dt} \quad (2.66)$$

$$j_{\text{SO}_4^{2-}} = \frac{V}{A_m} \frac{dC_{\text{SO}_4^{2-}}}{dt} \quad (2.67)$$

where  $A_m$  is the membrane area in  $\text{m}^2$ ,  $V$  is the begin volume of the reservoir where the flux of ions is going in or out in L and  $\frac{dC}{dt}$  is the concentration change over time. Since we will measure the concentration change over time, we can fit a linear model to the data to get  $\frac{dC}{dt}$ :

$$C(t) = C_0 + k \cdot t \quad (2.68)$$

$$\frac{dC}{dt} = k \quad (2.69)$$

where  $C_0$  is the initial concentration. When we have  $k$ , we can use equations 2.66 and 2.67 to get the corresponding fluxes.

After we have the flux of the ions we can define their transport numbers. This is defined as the ratio between the current carried by this ion and the total current [23]:

$$t_{\text{H}_2\text{PO}_4^-} = \frac{|z_{\text{H}_2\text{PO}_4^-}|j_{\text{H}_2\text{PO}_4^-}}{\sum z_i j_i} = \frac{1 \cdot j_{\text{H}_2\text{PO}_4^-}}{\sum z_i j_i} \quad (2.70)$$

$$t_{\text{SO}_4^{2-}} = \frac{|z_{\text{SO}_4^{2-}}|j_{\text{SO}_4^{2-}}}{\sum z_i j_i} = \frac{2 \cdot j_{\text{SO}_4^{2-}}}{\sum z_i j_i} \quad (2.71)$$

where the sum over the fluxes was defined by the current flow condition, Equation 2.20.

$$\sum z_i j_i = \frac{I_{DC}}{F} \quad (2.72)$$

The sum of the above transport numbers gives us the fraction of the current carried by the anions through the membrane,  $T_1$ . For the previous simulation, we used a  $T_1$  of 1, meaning that all the current was carried by anions. In reality however, there will always be an amount of co-ions being transported through the membrane. In our case, the cation is  $\text{Na}^+$ .

We can now define the permselectivity of phosphate with respect to sulfate [1]:

$$P_{\text{SO}_4^{2-}}^{\text{H}_2\text{PO}_4^-} = \frac{t_{\text{H}_2\text{PO}_4^-}/t_{\text{SO}_4^{2-}}}{|z_{\text{H}_2\text{PO}_4^-}|C_{\text{H}_2\text{PO}_4^-}/(|z_{\text{SO}_4^{2-}}|C_{\text{SO}_4^{2-}})} = \frac{j_{\text{H}_2\text{PO}_4^-} \cdot C_{\text{SO}_4^{2-}}}{j_{\text{SO}_4^{2-}} \cdot C_{\text{H}_2\text{PO}_4^-}} \quad (2.73)$$

where  $C$  indicates the average concentration in the feed solution during electro dialysis. This means an increase in  $P_{\text{SO}_4^{2-}}^{\text{H}_2\text{PO}_4^-}$  indicates a higher selectivity for phosphate over sulfate anions.

## 3. *Materials & Methods*

### 3.1. *Chemicals*

Demi water from built-in taps in the laboratories was used to prepare all solutions for the measurements. The conductivity was  $1.3 \mu\text{S cm}^{-1}$ . The following chemicals were used in preparing the solutions and modifying the membrane:

- Sodium phosphate monobasic monohydrate,  $\text{NaH}_2\text{PO}_4 \cdot \text{H}_2\text{O}$ .  $M = 137.99 \text{ g mol}^{-1}$ . (Sigma-Aldrich, assay 99.5%).
- Sodium chloride,  $\text{NaCl}$ ,  $M = 58.44 \text{ g mol}^{-1}$ . (Sigma-Aldrich, assay 99.8%).
- Sodium sulfate (anhydrous),  $\text{Na}_2\text{SO}_4$ .  $M = 142.02 \text{ g mol}^{-1}$ . (Fluka, assay 99%).
- Poly(sodium 4-styrene sulfonate), PSS. Average  $M_w \sim 70,000$ . (Sigma-Aldrich)
- Poly(diallyldimethylammonium chloride), PDADMAC. Average  $M_w \sim 300,000$ . (Sigma-Aldrich)
- Guanidine acetic acid, GAA.  $M = 117.12 \text{ g mol}^{-1}$ . (Sigma-Aldrich, assay 99%)
- Poly(allylamine hydrochloride), PAH. Average  $M_w \sim 15,000$ . (Sigma-Aldrich)

### 3.2. *Membrane Modification*

Membranes supplied by Fuji were used in this study. The bare AEM was a Fuji-AEM-80045 (Fujifilm Manufacturing Europe B.V., The Netherlands). We also used this type in the LbL modification. The membranes were first cut to fit the experimental setup and then stored in a salt solution before the modification was done. PAH-Gu was synthesized in the same manner as reported in the research by Cao et al [5].

For all 3 different PE modifications, we used PSS as the anionic layer. We dissolve 200 mg of PSS in 200 mL 0.5 M NaCl. The polycations (PDADMAC, PAH or PAH-Gu) were also dissolved in the same concentration of NaCl solution (the mass for all the other PEs was also 200 mg). The symmetric LbL modification is done by first completely immersing the bare membrane in 0.1 M of the PSS-NaCl solution for 10 minutes. Afterwards the membrane is rinsed off with Milli-Q water for 5 minutes. This is to ensure removal of weakly adhered polyelectrolytes. The membrane which is now coated with PSS is then immersed in a solution of PDADMAC, PAH or PAH-Gu for 10 minutes and afterwards rinsed off with water again. This process is repeated 2 times.

The end-result are 3 different symmetrically modified membranes with 2 bilayers of polyelectrolytes. They are identified as (PDADMAC/PSS)<sub>2</sub>, (PAH/PSS)<sub>2</sub> or (PAH-Gu/PSS)<sub>2</sub>. To prepare the asymmetric LbL modified membranes, the same procedure was applied. The only difference is that during immersion of the membrane in a PE solution, one side of the membrane is protected and not in contact with the solution.

### 3.3. Main Electrodialysis Setup

The setup used for EIS measurements and the electrodialysis is seen in Figure 3.1. It is composed of six chambers and made from plexiglass (STT Products, The Netherlands) [14].

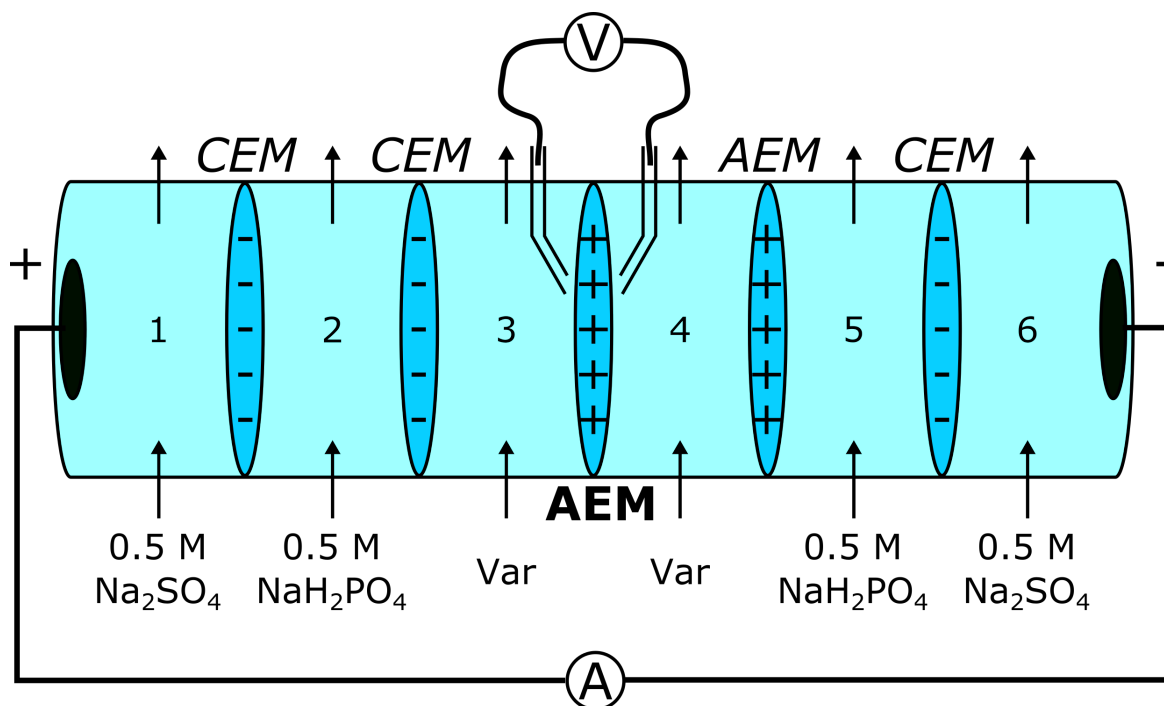


Figure 3.1: Overview of the measurement setup. CEM = Cation exchange membrane, AEM = Anion exchange membrane. Var stands for a variable salt solution composition and concentration.

The membrane we are investigating, is placed between chambers 3 and 4. It has an area of 8.04 cm<sup>2</sup>. The potential drop over the membrane is measured by Ag/AgCl electrodes attached to Luggin capillaries that are a few mm's away from the membrane surface. The capillaries are filled with the same solution as in their respective chambers. The

current through all the chambers is supplied by the working electrodes. They can be seen in black in the outermost cells (chambers 1 and 6). The cathode is made of stainless steel (negative during electro dialysis). The anode is made of platinized titanium (positive during electro dialysis), because we need an inert material to withstand the oxidation reactions. The configuration of the electrodes is known as the four-electrode setup [19]. It allows control of the current through all the membranes, while only measuring the potential drop over the main membrane. This is opposed to a two-electrode setup where the counter electrodes are also the measurement points for the potential.

It can be seen that besides the membrane under investigation, there are 4 others, separating the other cells. These auxiliary membranes have an area of 33.16 cm<sup>2</sup> (They're considerably larger than the membrane under investigation to make sure that the current is easily carried through these membranes). The placement of these membranes was based on the setup used by Krol et al. [29]. The chambers 1 and 6 are always supplied by a solution consisting of 0.5 M Na<sub>2</sub>SO<sub>4</sub>. This salt is chosen because it does not participate in the electrode reactions, which are [14]:

- Anode:  $2 \text{H}_2\text{O} \longrightarrow \text{O}_2 (\text{g}) + 4 \text{H}^+ + 4 \text{e}^-$
- Cathode:  $2 \text{H}_2\text{O} + 2 \text{e}^- \longrightarrow \text{H}_2 (\text{g}) + 2 \text{OH}^-$

Chambers 2 and 5 are supplied by a salt solution that has the same composition as the solution flowed past the membrane under investigation. We keep this concentration higher than the solution in chambers 3 and 4 to ensure that the concentration polarization that can occur, only happens at the central membrane.

The potentiometer and current source come from the same machine, an Autolab PGSTAT128N (Metrohm). It is a low current, entry-level, potentiostat/galvanostat capable of pushing 0.8 A between the counter electrodes at a maximum potential of 15 V. It is equipped with the FRA32M module for impedance analysis. All measurements have been made in galvanostatic mode, meaning that we control the current while measuring the potential drop across the membrane.

The 6 different reservoirs were all placed in a thermostatic bath at a controlled temperature of 25 °C. They were pumped through the chambers by 3 different peristaltic pumps. Chambers 1,2,5 and 6 were always flowed at a high speed of 110 mL min<sup>-1</sup>. The solution flow for the main chambers was different for the EIS measurements and the electro dialysis and is given in the corresponding section.

### 3.4. *EIS Setup*

For the impedance spectroscopy measurements we applied a direct current of  $I_{DC} = 0$  A. We investigated the impedance in the low frequency range from 1 Hz to 0.001 Hz. We are reluctant to increase the frequency too high because the impedance of the measuring electrodes becomes dominant in this regime and obtaining a reliable impedance of the membrane system becomes complicated (above 100 Hz the participation of the measuring electrodes becomes very noticeable) [45]. We used 20 frequency points, logarithmically divided. The current was oscillated with an amplitude of  $I_A = 5$  mA AC and integrated over 2 cycles for each frequency. We chose to have no DC bias for two reasons:

1. As explained in Section 2.5.7, the EEC is a more natural representation of the data if we don't polarize the layers.
2. The EIS measurements can take a very long time, due to the low frequencies. A measurement of just the 1 mHz impedance can take over half an hour. This means that the membrane needs to stay in the same steady state for multiple hours to analyze one EIS. This state can be easier maintained if we don't apply a DC bias.

The peristaltic pump for the solution next to the membrane was set at a flow rate of  $50 \text{ mL min}^{-1}$ . One 2 L bottle of solution with the desired salt concentration was used for both sides of the membrane. The pH of this solution was measured to ensure monovalent phosphate ions (always in the range 4.5-5). Furthermore, before the measurement, the setup was left to equilibrate for 30 min.

For each membrane under investigation, at least three runs were done for the whole frequency spectrum. The motivation behind this choice was based on the following reasons:

1. To study the repeatability of EIS measurements.
  - Even though there is a rich background literature on the subject of EIS in combination with IEM, there is very little material on the test–retest variability. Some papers only release data concerning fitting errors, which is not representative of the underlying principle [1].
  - We can also take the measurement error into account by repetition.
2. To investigate the effect of time and equilibrium processes on the IEM and how this effects the measured data.

A blank measurement is taken before and after the EIS. This gives us  $R_s$  which is later subtracted from the  $R_s + R_m$  value obtained from fitting to the EEC.

The data was fitted to an EEC with the help of ZView. The procedure for calculating the variable values with their corresponding errors can be found in Appendix C.

### 3.5. *Electrodialysis Setup*

The setup used for electro dialysis measurements is shown in Figure 2.13. A current density of  $7.5 \text{ mA cm}^{-2}$  is applied between the electrodes and through the membrane for 3 hours. It is first verified that this current is in the underlimiting, Ohmic regime. Samples (5 mL each) are collected from the receiving chamber (no. 3). The solution in the bottle is first rigorously stirred before extraction. One sample is then used to measure the concentration of both anions. All phosphate and sulfate containing solutions were analyzed through Ion Chromatography (930 Compact IC Flex, 150 mm A Supp 5 column, Metrohm).

## 4. Results & Discussion

### 4.1. Asymmetric vs Symmetric modification

After modifying three different membranes with the polyelectrolytes of interest we did EIS measurements with the setup that can be seen in Figure 3.1. A salt concentration of 0.1M  $\text{NaH}_2\text{PO}_4$  was used in the chambers that are in contact with the membrane under investigation. The Nyquist plot after two runs from an asymmetrically modified PAH-Gu membrane can be seen in Figure 4.1A. As explained in the methods section, multiple runs are done on a single membrane. In the case of asymmetrically modified membranes, we could not fit the EIS data to an EEC with an acceptable error.

In the case of PAH-Gu, we could not fit an EEC at all. It can be seen that the curves are erratic. When we switched to modifying the membranes in a symmetrical manner though, the curves were consistent with other theoretical and experimental research [41] [45] [50]. We were also able to fit them to the EEC with a very small error giving us a great deal of confidence in their accuracy. The curves and the fitted EEC curve can be seen on the right in Figure 4.1B.

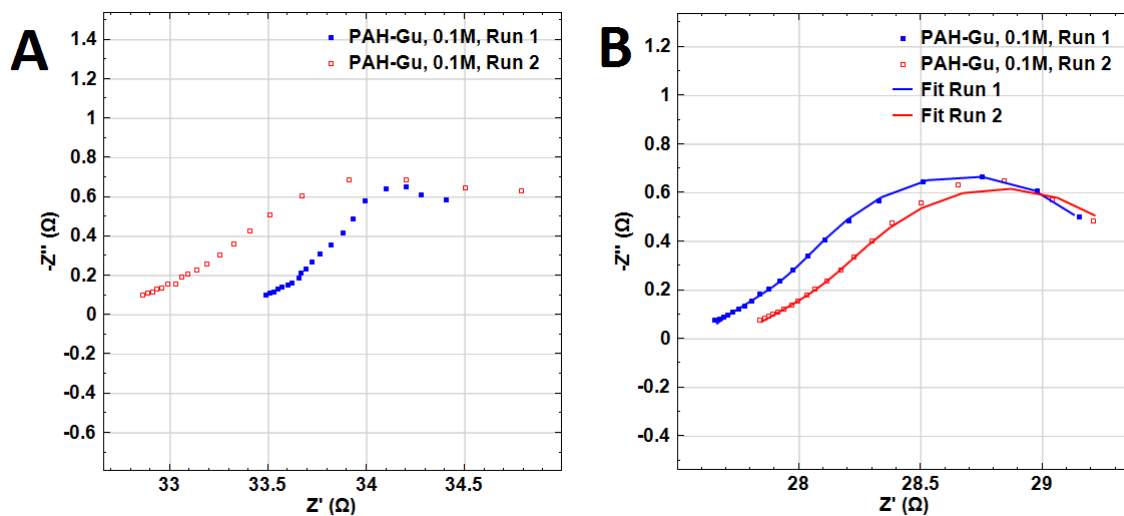


Figure 4.1: EIS measurements on PAH-Gu, LbL modified membranes. A) Asymmetric, data could not be fitted to the EEC and was very random and not reproducible. B) Symmetric, solid lines represent best fit to the EEC from Figure 2.12

Table 4.1: Fitting parameters to the EEC for asymmetric and symmetric LbL modified membranes. (Asym. PAH-Gu did not fit, so no parameters), R in  $\Omega \text{ cm}^2$ , C in F

Membrane Type		Chi-Sqr	$R_{\text{Membr.}}$	$R_{\text{EDL}}$	$C_{\text{EDL}}$	$R_{\text{DBL}}$	$\text{CPE}_{\text{DBL-n}}$	$\text{CPE}_{\text{DBL-Q}}$
Bare AEM		9.31E-6	34.5	6.80	88.5	8.05	0.43	3.46
Asym.	PDADMAC	1.14E-05	50.00	8.54	81.2	15.16	0.35	2.4
	PAH	1.66E-03	26.5	0.95	75.9	8.49	0.34	2.387
	PAH-Gu	-	-	-	-	-	-	-
Sym.	PDADMAC	8.86E-6	33.61	5.57	103.3	7.67	0.45	3.74
	PAH	3.86E-5	30.31	5.63	115.1	9.07	0.43	3.43
	PAH-Gu	1.11E-5	29.1	6.34	105.3	8.08	0.47	3.85

The comparison in fitting parameters for asymmetrically and symmetrically modified membranes can be seen in Table 4.1. For the asymmetric PDADMAC, the error was low due to convergence in the fitting process, though the values of the equivalent components were not realistic (e.d. a membrane resistance of  $50 \Omega \text{ cm}^2$ ). In the case of asymmetric PAH, the fitting error was very high due to erratic curves in the Nyquist plot. The symmetrically modified membranes though have a low error by exhibiting consistent behavior over multiple measurement runs. Furthermore, the fitted equivalent elements are in agreement with each other. For example, previous theoretical research showed that modifying the membrane with polyelectrolytes should not have an effect on the DBL layers [16] [1]. This has experimentally been confirmed since the values for  $R_{\text{DBL}}$  and the  $\text{CPE}_{\text{DBL}}$  stay the same for the modified and the bare membranes.

We can identify a few reasons that explain why we were not able to fit the EIS data obtained from asymmetrically modified membranes to an EEC:

1. There may have been a detachment of the polyelectrolyte layer. This could explain the erratic behavior between consecutive measurements on the same membrane.
2. The EEC was not a good representation of the layers that are created near the membrane surface.
  - Analytical calculations on the low-frequency impedance by Nikonenko [45] show that the impedance spectra will have a deviating shape when there is a difference in the characteristics of the layers on either side of the membrane. The curve that the asymmetrically modified membranes exhibit (example in the left side of Figure 4.1), show a resemblance to theoretical impedance

spectra calculated with a difference in DBL thickness on either side of the membrane.

- This would only explain a single measurement run, not the inconsistency between multiple runs.
3. A consistent flaw in the preparation of the asymmetric layers. Since we only modify one side of the membrane, the complexity of coating the membrane increases and can lead to a problem in the formation of the polyelectrolyte layer. For example, it could be that the side of the membrane that is protected during the LbL modification gets damaged in some way and therefore the transport characteristics are skewed.

The following research will be conducted by using symmetrically modified AEM membranes since this method yields consistent and reproducible results that can be fitted to an EEC with high accuracy.

## 4.2. *Electrochemical Impedance Measurements*

We continue with the EIS measurements on the modified and bare membranes, but now for a wider concentration range of  $\text{NaH}_2\text{PO}_4$ . We did multiple measurements on each membrane type for each concentration until we had at least three consecutive measurements of which the impedance spectra did not change. This led to a lower error for fitting the measurement data to the EEC. In the following four figures, you can find the fitted values of the different components for each modified and unmodified membrane, for a range of solution salt concentration.

### 4.2.1 Membrane Resistance

Figure 4.2 shows the value of the  $R_m$  component in the EEC, for different concentrations.

We start with the low concentration regime, 0.1M  $\text{NaH}_2\text{PO}_4$ . To make the overview clearer, a bar graph can be found in Figure 4.3a. We can see that for these concentrations the lowest membrane resistance is achieved with the PAH-Gu modified membrane, around  $29 \Omega \text{ cm}^2$ , which is a drop of almost 15% when compared to the bare membrane. The obvious explanation would be a confirmation of the hypothesis that Guanidinium has a positive effect on transport resistance of phosphate anions. Due to the interactions between Guanidinium and phosphate in the added layers, the anions have an easier passage through the membrane complex.

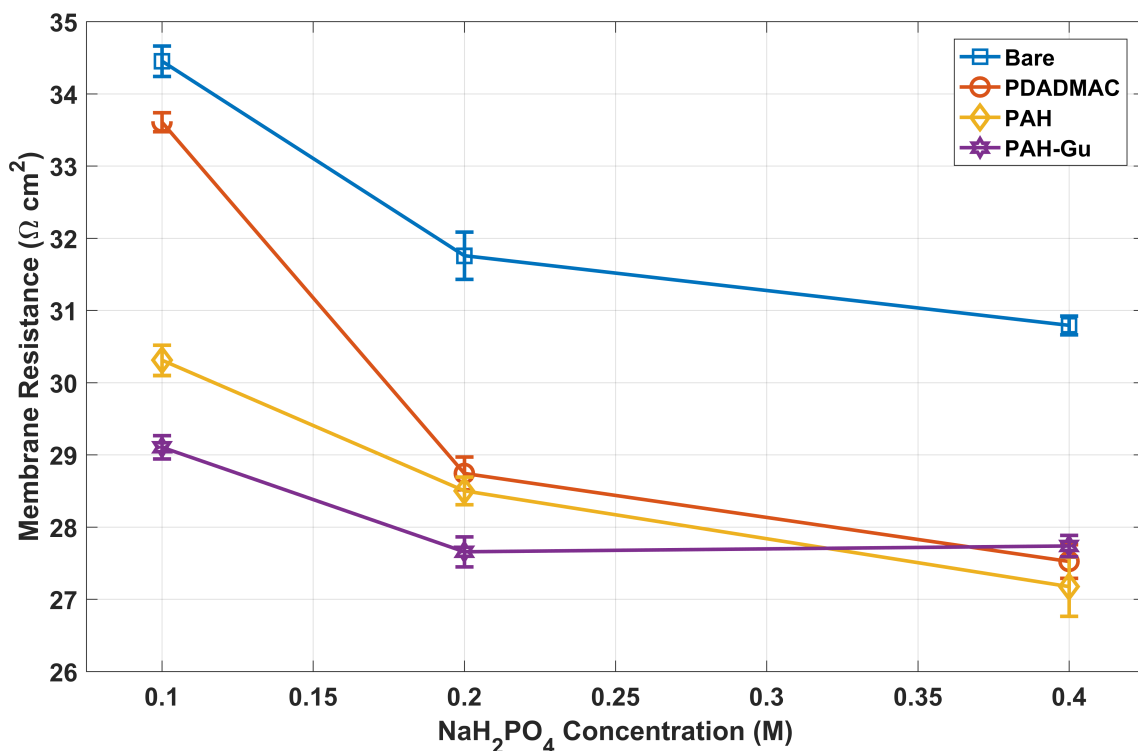


Figure 4.2: Membrane resistance obtained from the EEC for different solution concentrations. (Lines serve as guide only, measurement points indicated)

The difference in resistance of the membranes is the highest for low concentrations. This was also previously noted in other experimental research with different salts [11]. An explanation for this phenomenon is not conclusive yet, although a model by Galama et al. showed that modeling the membrane as a structure of micro-cavities and -channels in serial order can explain this behavior [20].

The PAH membrane has a slightly higher resistance than its Guanidinium modified counterpart. An interesting feature is the similarity in resistance between PDADMAC and the bare membrane. There is only  $1 \Omega \text{ cm}^2$  difference. Since the charged groups of PDADMAC resemble those of the bare membrane, their resistances are close, apparently.

A bar graph of the high concentration region is found in Figure 4.3b. It is revealed that the type of LbL modification does not matter for a high concentration solution. All the modified membranes had a resistance around  $27.5 \Omega \text{ cm}^2$ , while the bare membrane's resistance was around 10% higher. The convergence of the resistance for the modified membranes can be explained as followed: Since we added more charge to the membrane,

the anions are more attracted to the larger charge. This facilitates transport. Because there is a large amount of anions for the high concentration regime, the interaction between anions and the specific fixed-charged groups becomes less important.

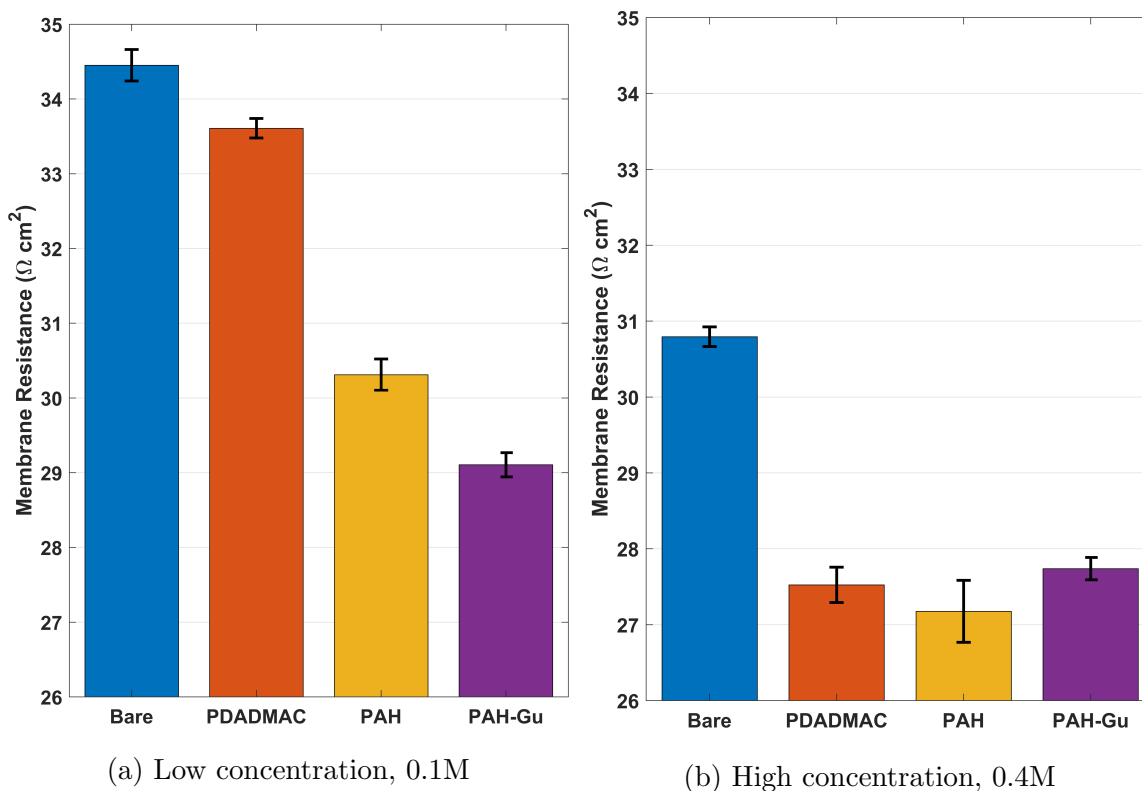


Figure 4.3: Bar graph of the membrane resistances with a phosphate solution

## 4.2.2 DBL Impedance

The constant phase element fitting showed no difference between the membrane types (typical values can be seen in Table 4.1). Therefore we will only focus on the resistance of this circuit. The resistance for the DBL can be seen in Figure 4.4. As stated in Section 2.4.3 the resistance of this layer is mainly caused by the flow and composition of the solution next to the membrane. This was another motivation to take the DBL circuit into account during the EEC fitting process.

The PAH modified membrane showed the highest resistance, though this can be written off on the high fitting error with the EEC. When compared to the differences noted in the membrane resistance section, the differences between membrane types for this variable, are negligible.

The overall, average DBL resistance for all membranes starts around  $8 \Omega \text{ cm}^2$  for 0.1M. If we increase the concentration to 0.4M, we don't see a linear decrease following this trend. For this high concentration, the resistance reaches an apparent equilibrium around  $4 \Omega \text{ cm}^2$ . This infers that at a high salt concentration the construction of a DBL is inhibited. This was previously noted for salts with a high diffusion coefficient [46], but is now also confirmed for the low mobility phosphate anions.

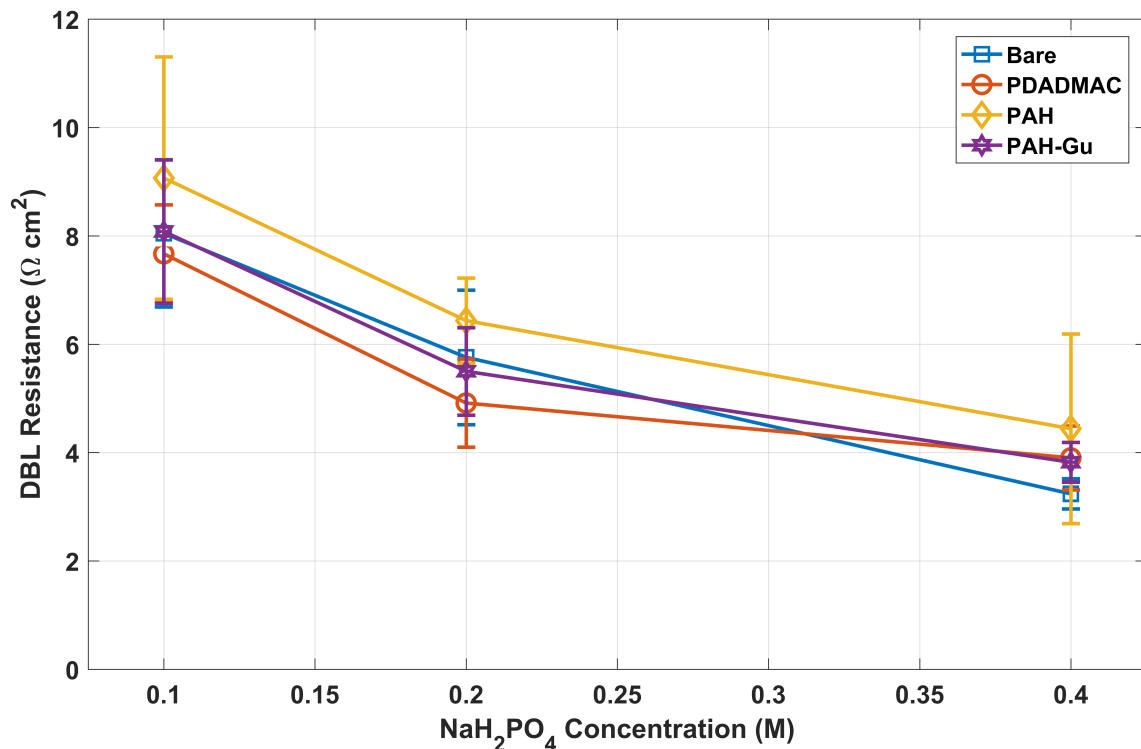


Figure 4.4: DBL resistance obtained from the EEC for different solution concentrations. (Lines serve as guide only, measurement points indicated)

### 4.2.3 EDL Impedance

The resistance of the EDL component in the EEC can be seen in Figure 4.5 for the concentration range. As was the case for the DBL resistance, no clear difference can be seen between the different membrane types. We do notice a rapid decline when we increase the salt concentrations. At 0.1M the resistance for all membranes is around  $6 \Omega \text{ cm}^2$ . At a high concentration of 0.4M though, the resistance of the EDL seems to become increasingly negligible. This is explained by the Donnan potential at the

surface, Equation 2.39. Because the concentration at the solution/membrane interface comes close to the concentration in the membrane, there is no potential difference anymore, and so no resistance.

The capacitance of the EDL component in the EEC can be seen in Figure 4.6. Just as with the EDL resistance, the equivalent capacitance of this layer shows no significant difference between the four types of tested membranes. Noteworthy, here is the non-linear increase in capacitance as a function of salt concentration. The Debye length, Equation 2.38, decreases with an increase of concentration. Since this means that the double layer thickness also decreases by this factor, we have an increase in capacitance (capacitance is proportional to the inverse of charge distance separation).

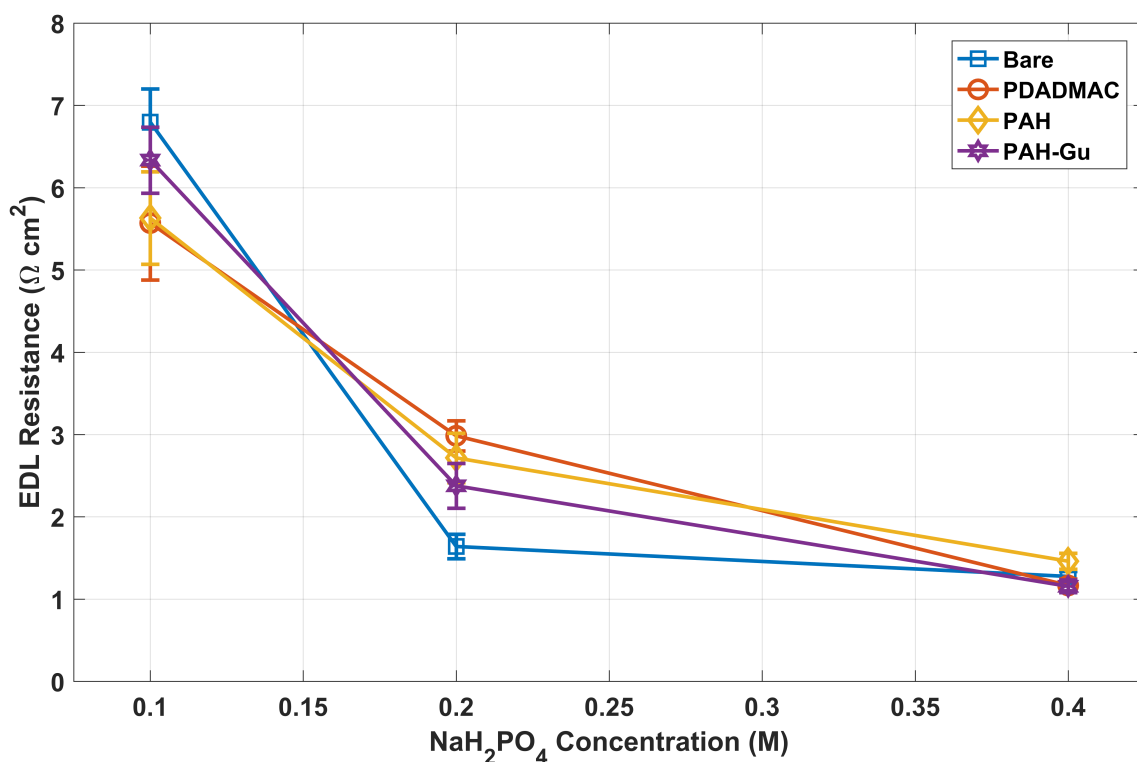


Figure 4.5: EDL resistance obtained from the EEC for different solution concentrations. (Lines serve as guide only, measurement points indicated)

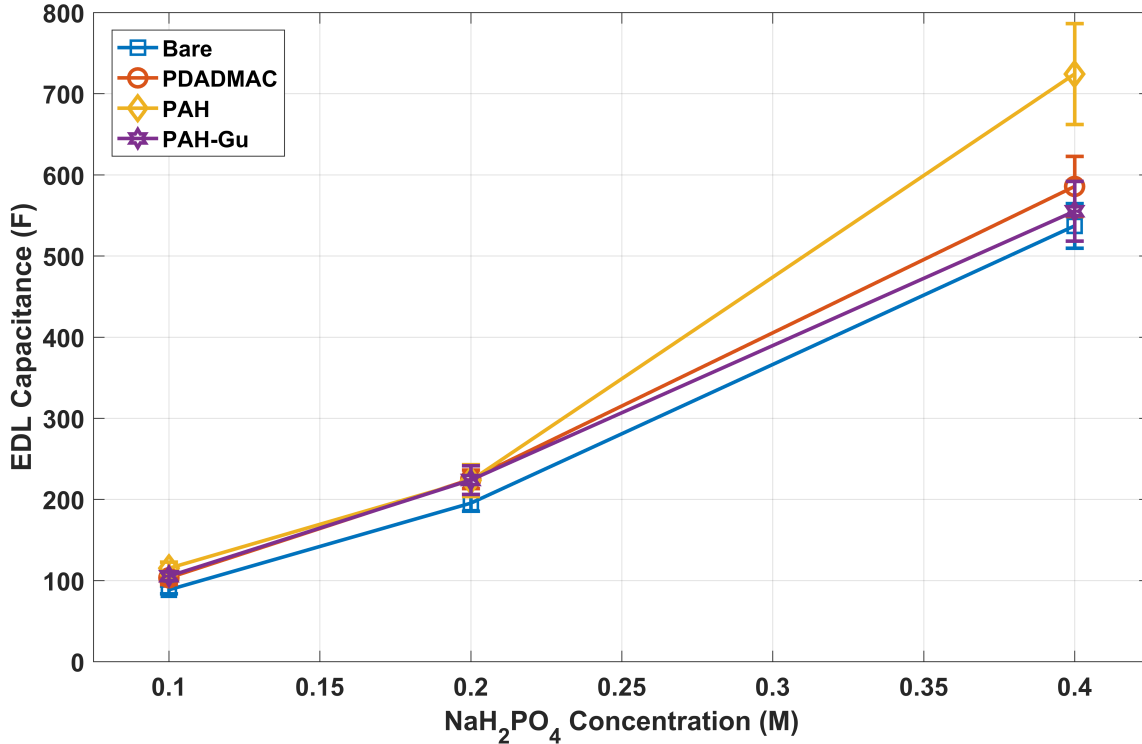


Figure 4.6: EDL capacitance obtained from the EEC for different solution concentrations. (Lines serve as guide only, measurement points indicated)

### 4.3. *Electrodialysis*

After the characterisation of the membranes, we will now perform electrodialysis. Now that it is confirmed that phosphate anions face a lower membrane resistance with the modified membranes when compared to the bare, we want to investigate if the transport of phosphate is preferred when there is a competing anion. The ED is performed with a mixed solution of phosphate and sulfate, as shown in Figure 2.13. The concentration of both salts is set at 0.025 M. We chose the low concentration regime because this is where the difference in membrane resistance is most noticeable, as seen in the previous results. A current density of  $7.5 \text{ mA cm}^{-2}$  was applied, which is about 70% of the limiting current density. As mentioned previously, a sample was taken from the receiving solution every 30 minutes. In Figure 4.7 the concentration of phosphate anions in the receiving chamber can be seen over a time period of 3 hours during electrodialysis. The simultaneous concentration of sulfate anions can be seen

in Figure 4.8. Upon visual inspection of the phosphate and sulfate concentration over time, we first notice that there is a large drop in concentration for the PDADMAC modified membrane in the first two measurement points. This might be due to a sample collection error, since it occurred for both anions (one sample is used to measure the concentration of both anions.). The solution might not have been stirred properly before removal of a sample. We cannot perceive more than these large scale tendencies with the bare eye from the graphs. So now we turn to calculations for further analysis.

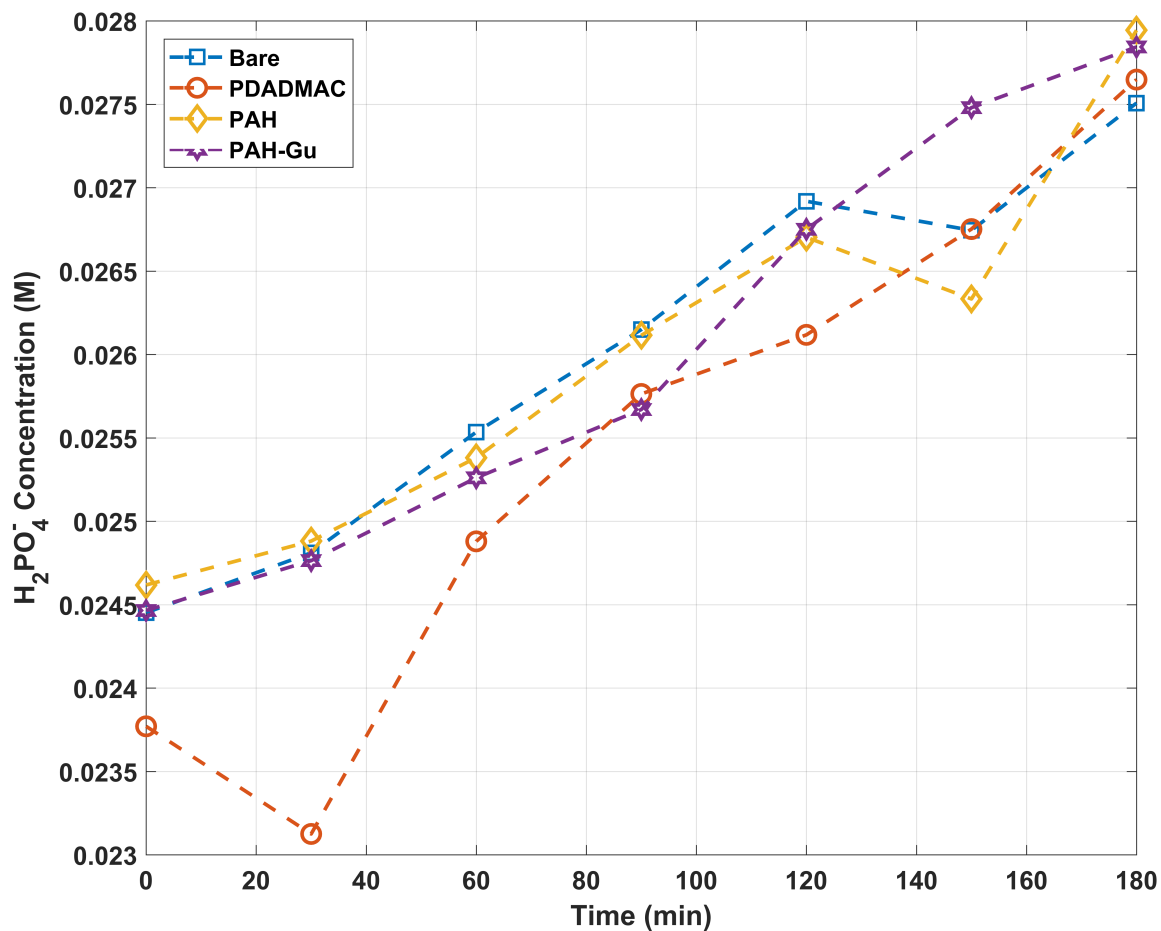


Figure 4.7:  $\text{H}_2\text{PO}_4^-$  concentration over time in the receiving chamber. (Lines serve as guide only, measurement points indicated)

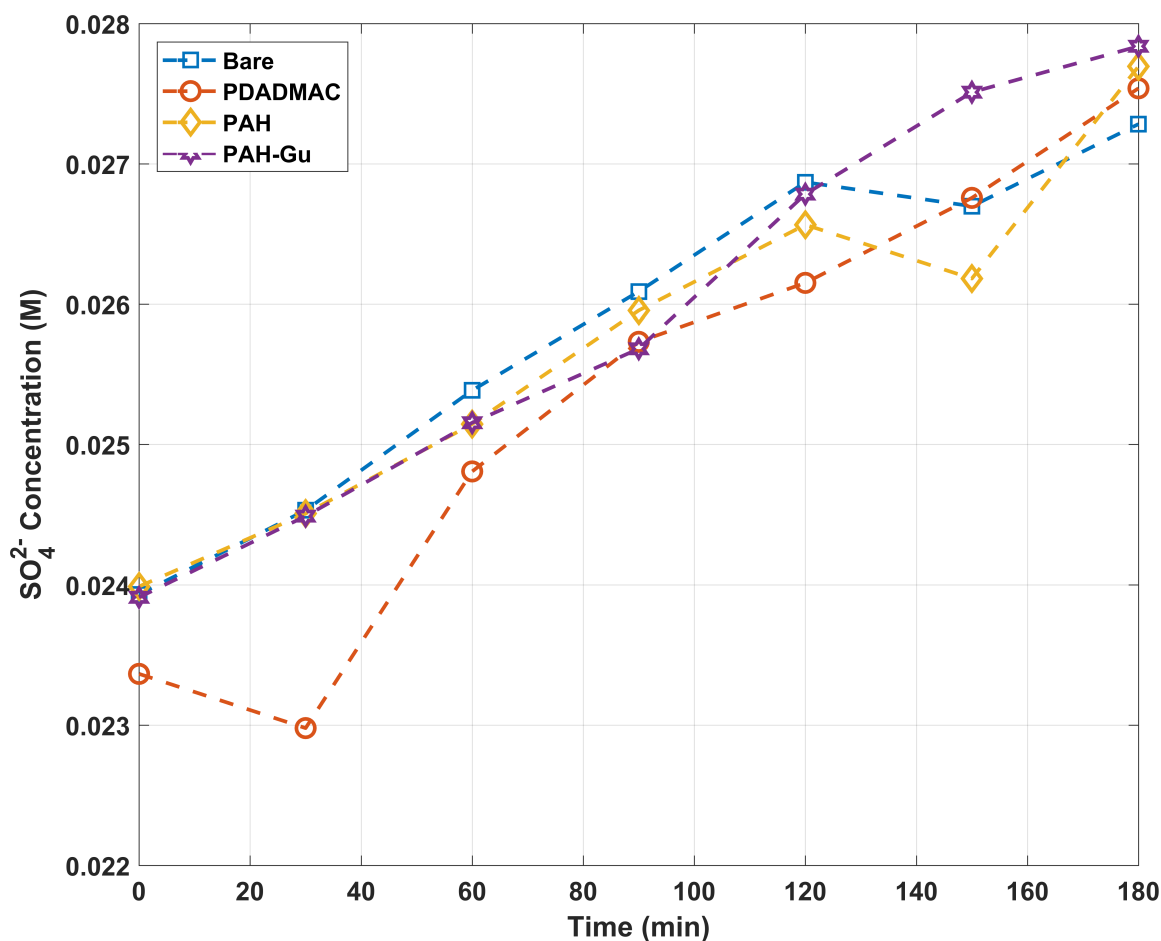


Figure 4.8:  $\text{SO}_4^{2-}$  concentration over time in the receiving chamber. (Lines serve as guide only, measurement points indicated)

We first calculate the flux of both anions by use of Equations 2.66 and 2.67 and fitting a linear model to the data as in equation 2.68 (fitting parameters can be found in Appendix D). The total flux of the anions can then be related to the applied current density to get the total amount of current carried by the anions. These values can be seen in Table 4.2.

It is first noted that the flux of sulfate is always higher than that of phosphate, independent of the membrane. A slight increase of sulfate transport is to be expected for the bare membrane, since the diffusion coefficient of  $\text{SO}_4^{2-}$  is higher than that of  $\text{H}_2\text{PO}_4^-$ .

The flux of phosphate anions is the highest with the PAH-Gu membrane at  $1.82 \cdot 10^{-8} \text{ mol cm}^{-2} \text{ s}^{-1}$ . The effective transport of anions is also the highest for PAH-Gu. With

this membrane, 81% of the current is carried by the anions. This can be explained because the membrane resistance in this low concentration regime is significantly below that of the other membranes, so at least the phosphate flux will be higher, and in this case the sulfate flux as well. The PDADMAC modified membrane has the lowest flux of anions. A reason for this behavior might lie in the high charge density of this membrane.

Table 4.2: Flux of anions and percentage of current carried by both anions combined for ED of 0.025M  $\text{H}_2\text{PO}_4^- + \text{SO}_4^{2-}$ ,  $7.5 \text{ mA cm}^{-2}$ .

Membrane	Flux $\text{H}_2\text{PO}_4^-$ ( $10^{-8} \text{ mol cm}^{-2} \text{ s}^{-1}$ )	Flux $\text{SO}_4^{2-}$ ( $10^{-8} \text{ mol cm}^{-2} \text{ s}^{-1}$ )	Percentage of current carried by anions
Bare	1.71	2.00	74%
PDADMAC	1.47	1.83	66%
PAH	1.69	1.93	72%
PAH-Gu	1.82	2.21	81%

After we have the flux of each anion specie, we can use Equations 2.70 and 2.71 to arrive at the transport numbers. We can finally calculate the permselectivity of each membrane type, Equation 2.73. These values can be found in Table 4.3.

Since all the permselectivity values are lower than 1, this implies that the sulfate anions are more easily transported through the membranes. Interestingly enough, the permselectivity of the PAH-Gu membrane is actually a little bit lower than the bare membrane, 0.83 against 0.85 respectively. On the other hand, the PAH modified membrane had the highest discriminatory function for phosphate over sulfate, with a permselectivity of 0.88. This is a clear indication that modifying a membrane with Guanidinium actually **reduces** the selectivity for phosphate over sulfate. The reason behind this unexpected outcome might have multiple causes.

1. The interaction between phosphate anions and the Guanidinium enriched layers could be too strong. This might give the sulfate anions priority in the current transport.
2. A change of the pH-level in or near the membrane, might change the valence of the phosphate anions [49].

Table 4.3: Transport numbers and permselectivity for ED of 0.025M  $\text{H}_2\text{PO}_4^- + \text{SO}_4^{2-}$ ,  $7.5 \text{ mA cm}^{-2}$ .

Membrane	Transport number $\text{H}_2\text{PO}_4^-$	Transport number $\text{SO}_4^{2-}$	Permselectivity $P_{\text{SO}_4^{2-}}^{\text{H}_2\text{PO}_4^-}$
Bare	0.22	0.52	0.85
PDADMAC	0.19	0.47	0.80
PAH	0.22	0.50	0.88
PAH-Gu	0.24	0.57	0.83

## 5. *Conclusion*

### 5.1. *Asymmetric vs Symmetric LbL*

It was shown that for the asymmetric LbL modification method, the EIS measurements yielded inconsistent results. The data also did not fit to our EEC. The symmetric method however, gave better results and was fitted to an electrical equivalent circuit. The EEC was determined from literature and theoretical impedance calculations. Because of the uncertainty in the acquired data gained with the asymmetric method, we decided to proceed with the symmetrically modified membranes. Reasons for the disappointing results with the asymmetric technique included: Detachment of the layer, wrong EEC analog or bad preparation of the layers.

### 5.2. *Electrochemical Impedance Measurements*

The most important result lies in the membrane resistance. As previous research with different salts and membranes showed, the membrane resistance is the highest for low concentration regions [11]. In the 0.1 M region, the PAH-Gu modified membrane had the lowest resistance of all 4 tested membranes ( $29 \Omega \text{ cm}^2$ ), including the bare, unmodified membrane ( $34.5 \Omega \text{ cm}^2$ ). This can be attributed to the selective interaction between phosphate and Guanidinium [5]. PDADMAC showed a resemblance to the bare membrane in the low concentration region due to similarities of the fixed charged groups.

For high concentrations though, the difference between modified and unmodified membranes is less reliant on the specific PE used for LbL modification. All the modified membranes had a similar resistance, lower than the bare membrane's (about 10% lower). This was probably due to more charge on the membrane.

As expected, the DBL and EDL resistances were the largest for low concentrations. It was previously hypothesized that in this low concentration region, the DBL and EDL contributions to the overall resistance were large, and this was confirmed for phosphate [19]. Furthermore, we have found that for a phosphate solution, the EDL resistance drops very rapidly for an increase in concentration. The capacitance of the EDL was significantly increased for higher salt concentrations. This indicates a decrease in charge separation in the electric double layer near the membrane surface, which can be explained by a decrease in the Debye length.

### 5.3. *Electrodialysis*

Electrodialysis was performed with a mixed solution of phosphate and sulfate to determine permselectivity. It was shown that the Guanidinium modified membrane had the highest flux of phosphate and sulfate anions and the highest effective transport number for anions,  $T_1$ , with a value of 0.81. The bare membrane's  $T_1$  was measured at 0.74.

All membranes had a permselectivity lower than 1, meaning that there was no preference for phosphate transport over sulfate. The permselectivity was lowered for PAH-Gu, 0.83, when compared to the bare membrane, 0.85. The bare membrane and the PAH modified membrane both had a higher discriminatory function than the Guanidinium modified membrane. This indicated that modifying a membrane with Guanidinium does not increase the permselectivity for phosphate of sulfate, even though it does increase the overall anion transport number. The decrease in phosphate permselectivity against sulfate might stem from an interaction between the Guanidinium and phosphate which is too strong when compared to sulfate and therefore lowers the permselectivity.

The increase in flux of anions when modifying an AEM with PAH-Gu of 10% when compared to a bare membrane, is promising though, and justifies further research in this direction.

## 6. *Outlook*

In this section I'd like to make a few suggestions for future research:

- The electro dialysis results might be improved by replacing the AEM between chambers 4 and 5 with a CEM. This way we can increase the anion independence in chambers 3 and 4 of our setup (receiving and feed solutions respectively). In an ideal case, the concentration drop of anions in our feed solution will give an equal increased amount in the receiving solution.
- It was found that the selectivity for phosphate when compared to sulfate was not influenced by modifying our membranes with the layer-by-layer method (measured with electro dialysis at high current densities). Instead of looking at other modifications to the membrane, we could use a different competing anion. It was shown in the work by Cao that the sulfate anions also had a certain weak binding to the Guanidinium [5]. It was also found that chloride anions had no interaction with the Guanidinium. To test the hypothesis that Guanidinium should have a positive effect on the selective transport of phosphate, we can use chloride, nitrate or organic anions as a competing anion. Since chloride does have a substantially higher diffusion coefficient, we need to carefully check against a bare membrane for reference.
- We didn't investigate membrane resistance for phosphate concentrations lower than 0.1 M, but recent research by Sarapulova et al. reported unusual resistance values in this regime with different IEMs [49]. They described a decrease of resistance for further dilution of the solution,  $<0.04$  M. It would be interesting to see if this tendency is also observed with the AEM used in this research.
- In this study we characterized the membranes with the EIS method. We used 0 A direct current though. All the theoretical research though, was based on the assumption that a DC was applied to polarize the layers and transport counterions [50]. In that previous research the EIS was introduced by overlaying a low current, low frequency oscillation over the DC. By characterizing the membrane in this phase you can assess the actual resistances during transport. These might differ from the resistances we measured with 0 A DC, because in this state there was no large polarization and no net transport of counter ions.
- It was reported in the early 70's that applying an cationic layer on top of an CEM could increase the monovalent selectivity [53]. This is due to the repulsive effect on divalent ions. The same method was recently applied to AEMs by placing a

layer with strong negative charge on top of the membrane [22]. The monovalent anion selectivity went up. If the binding of Guanidinium proves to be too strong and does not increase the transport of phosphates, then this procedure might be an alternative in case divalent ions are used as competing anions (e.g. sulphate)

- A more robust measuring method for the electrodialysis must be found. At the moment it is hard to estimate measurement uncertainties cause there are too many variables that can have a large effect on the outcome, such as thorough mixing of the solutions and sample collection methods.
- The amount of literature in this field is nothing short of mind-boggling. This huge background however, gives us a very fragmented view on the subject. For a variable as the membrane resistance, there are already at least 4 different measurement methods that have little in common with each other. There is the direct current method where the resistance is determined by the potential drop over the entire IEM system and calculated via Ohm's law. One of the more reliable methods is high frequency (HF) impedance spectroscopy where it is assumed that we only measure membrane (and bulk solution) resistance for HF oscillations. Besides the different methods, the experimental setup also differs between research. Some researchers use a two-electrode setup, which can give false results due to interference reactions at the working electrodes. Others (like in this research), deploy a four-electrode setup, which is more reliable due to none or negligible side-effects from electrode reactions. This procedure though is more complicated and has a lot more variables that also vary between studies.

For this reason, it is proposed by a few to make measurement methods more consistent with each other. By choosing this road, it will become easier to exchange data between colleagues and analyze your data against a more comprehensive database of results by others. For example, the method introduced by Galama et al. has a promising future as becoming the standard procedure in determining membrane resistance due to its many advantages. such as reliability and consistency [19].

## A. Integral with complex arguments

Matlab (and other related software such as Scilab) is not able to evaluate integrals involving hyperbolic functions with complex arguments (Equations 2.58 and 2.59). Therefore we need to rewrite the integrals. We start with the following variable change:

$$X = \frac{x}{\delta_1} \quad (\text{A.1})$$

The integral we want to evaluate then becomes:

$$\int_0^1 \frac{\sinh(\alpha X)}{(1 - \beta X)^2} dX = \frac{1}{2} \left( \int_0^1 \frac{e^{\alpha X}}{(1 - \beta X)^2} dX - \int_0^1 \frac{e^{-\alpha X}}{(1 - \beta X)^2} dX \right) \quad (\text{A.2})$$

In the paper by Sostat et al. they used an approximation with the exponential integral function [50]. I found this method to be extremely cumbersome and it did not yield the correct result for certain input variables. I therefore used the following approach to calculate the integral. By using Euler's formula we can split the first integral on the right side of Equation A.2 into:

$$\int_0^1 \frac{e^{X \operatorname{Re}\{\alpha\}} (\cos(\operatorname{Im}\{\alpha\} X) + i \sin(\operatorname{Im}\{\alpha\} X))}{(1 - \beta x)^2} dX \quad (\text{A.3})$$

Applying the same method to the other integral in A.2, we can rewrite the whole as:

$$\int_0^1 \frac{\cos(\operatorname{Im}\{\alpha\} X) (e^{X \operatorname{Re}\{\alpha\}} - e^{-X \operatorname{Re}\{\alpha\}})}{(1 - \beta x)^2} dX + i \int_0^1 \frac{\sin(\operatorname{Im}\{\alpha\} X) (e^{X \operatorname{Re}\{\alpha\}} + e^{-X \operatorname{Re}\{\alpha\}})}{(1 - \beta x)^2} dX \quad (\text{A.4})$$

Matlab [37] has a built-in function to separate the real and the imaginary parts of a complex number and can evaluate the above real-valued integrals.

## B. *EIS Raw Data*

To give an impression of the data acquisition process, a plot of the raw data after three consecutive runs with a PDADMAC modified membrane in 0.4M phosphate, can be seen in Figure B.1. The measurements are repeated, until there is convergence of the characteristic curve.

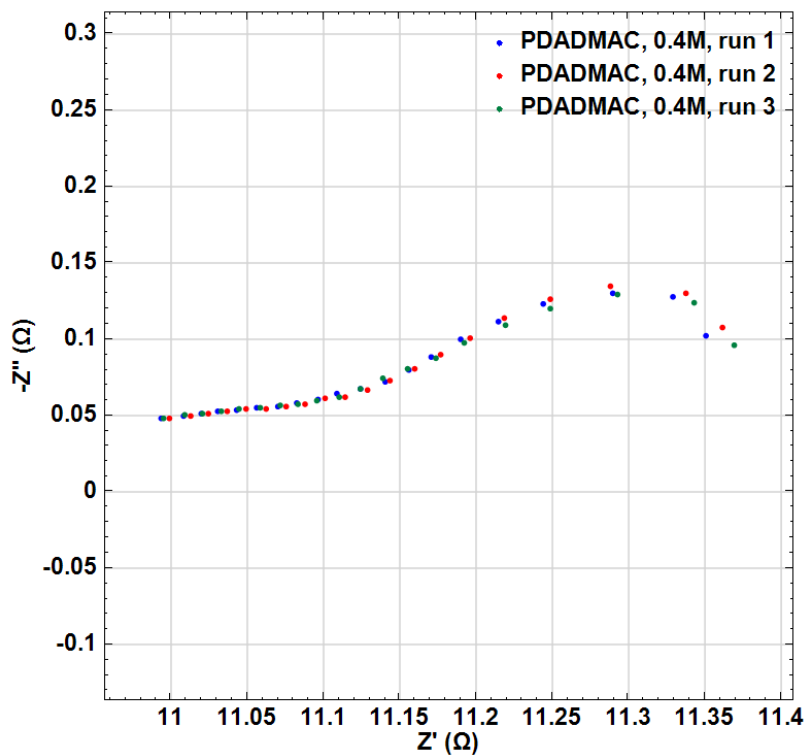


Figure B.1: Three consecutive data runs with a LbL modified membrane

This is done for all the membrane types and concentrations. The data is then exported to Zview for further analysis and fitting to the EEC.

## C. Fitting to the EEC

We imported the data from Nova (Metrohm B.V. [39]) to ZView 2 (Version 3.2b [24]). In this program, maintained by Scribner Associates, we fitted the following model to our data:

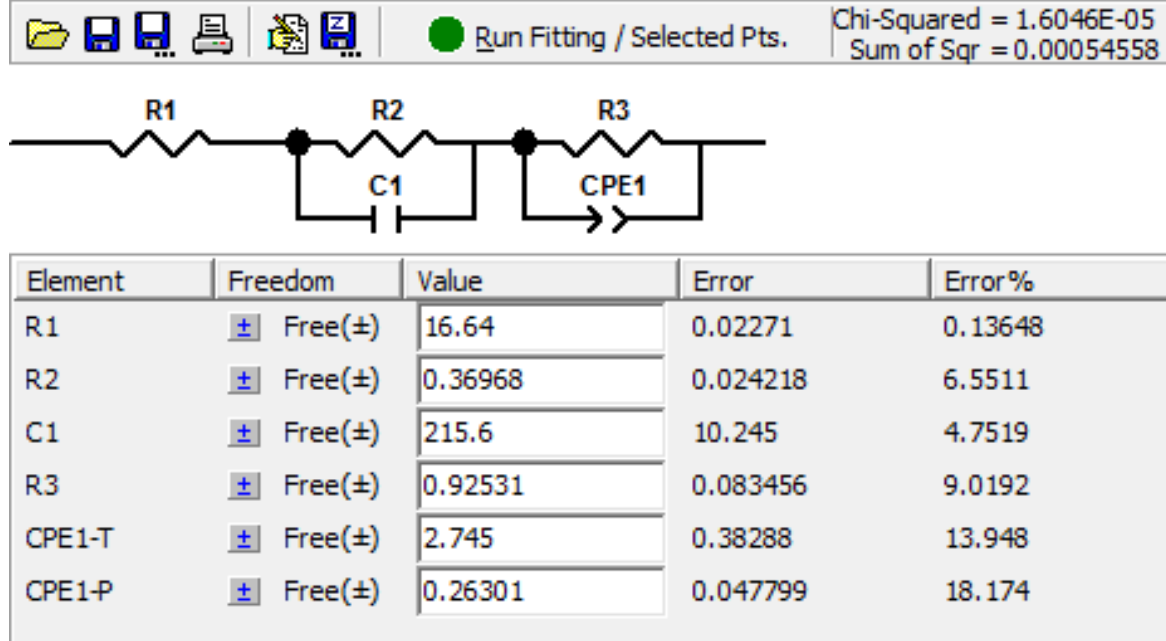


Figure C.1: Parameters from fitting EIS to an EEC model in ZView 2.0

As with all fitting we looked for starting values that gave the smallest error in the end-result. In this program the error was measured by the Chi-Squared. This value is the square of the standard deviation between the original data and the calculated spectrum. We then visually confirmed if the fitting was appropriate by looking at the Nyquist plot comparison (Figure C.2) and the frequency Bode plot (Figure C.3). In all the Figures in the Results chapter we can find the variable values, denoted here by  $p$ , and their error bars, denoted here by  $\sigma$ . If we define the values found by Zview with  $p_i$  ( $i = 1, 2, 3$  for the three consecutive runs) and their Chi squared error by  $X^2$ , we can find  $p$  and  $\sigma$  by minimizing the following equation:

$$\sigma^2 = \sum_{i=1}^3 \frac{(p_i - p)^2}{X^2} \quad (\text{C.1})$$

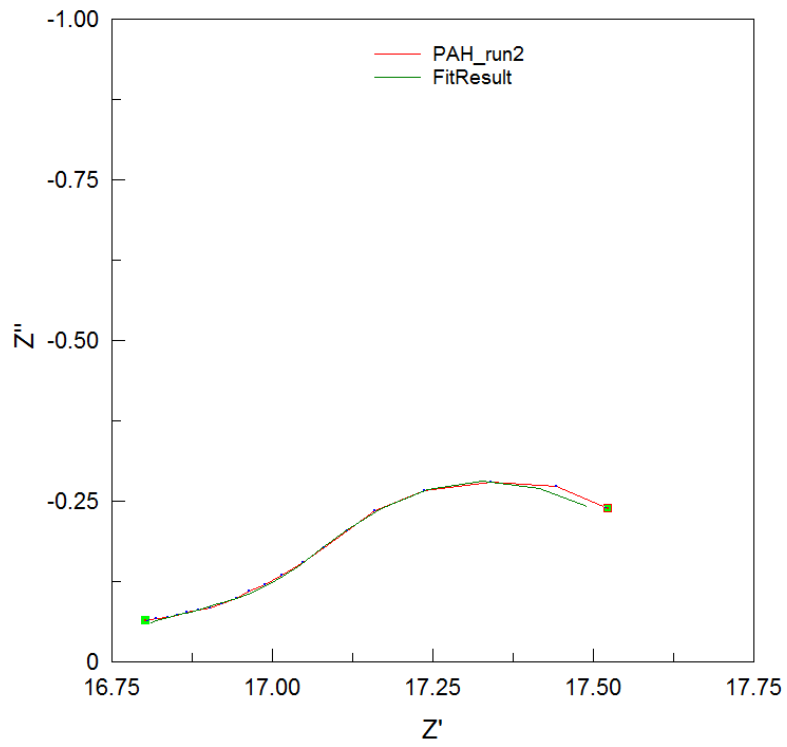


Figure C.2: Nyquist plot of experimental data overlaid with fitted EEC model in ZView 2.0

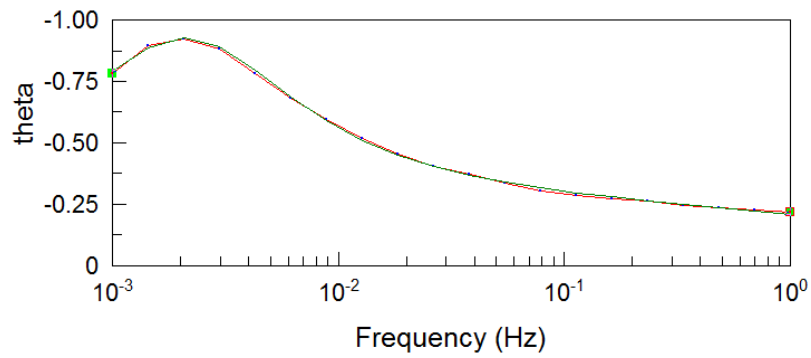


Figure C.3: Bode plot of experimental data overlaid with fitted EEC model in ZView 2.0

## D. *Linear model fitting to ED data*

The concentration over time data (Figures 4.7 and 4.8) were fitted to the model in Equation 2.68. Matlab was used and a linear least squares method was applied.  $C_0$  of 0.0245 was taken for the  $\text{H}_2\text{PO}_4^-$  concentration fitting and 0.024 for the  $\text{SO}_4^{2-}$  concentration.

Table D.1: Fitting parameters used on the data in Figures 4.7 and 4.8. Values in  $10^{-7}$   $\text{mol L}^{-1} \text{s}^{-1}$ .

Membrane	$k_{\text{H}_2\text{PO}_4^-}$	$k_{\text{SO}_4^{2-}}$
Bare	2.824	3.312
PDADMAC	2.429	3.017
PAH	2.785	3.175
PAH-Gu	3.007	3.637

# *Nomenclature*

## **Abbreviations**

IEM	Ion Exchange Membrane
AEM	Anion Exchange Membrane
CEM	Cation Exchange Membrane
PE	Polyelectrolytes
PEM	Polyelectrolyte Multilayer
PSS	Poly(sodium 4-styrene sulfonate)
PDADMAC	Poly(diallyldimethylammonium chloride)
PAH	Poly(allylamine hydrochloride)
PAH-Gu	Poly(allylamine hydrochloride)-Guanidinium
LCD	Limiting Current Density
BDL	Boundary Diffusive Layer
EDL	Electrical Double Layer
EIS	Electrochemical Impedance Spectroscopy
BC	Boundary Condition
AC	Active Current
DC	Direct Current
NP	Nernst-Planck

## **Physics Constants**

$\epsilon_0$	Vacuum permittivity	$8.8 \cdot 10^{-12} \text{ F m}^{-1}$
$e$	Elementary charge	$1.6 \cdot 10^{-19} \text{ C}$
$F$	Faraday constant	$96,485 \text{ C mol}^{-1}$

$k_B$	Boltzmann constant	$1.38 \cdot 10^{-23} \text{ m}^2 \text{ kg s}^{-2} \text{ K}^{-1}$
$R$	Gas constant	$8.3 \text{ kg m}^2 \text{ s}^{-2} \text{ K}^{-1} \text{ mol}^{-1}$

### Symbols

$\beta$	Ratio of DC to LCD
$\eta$	Electrochemical Potential
$\lambda$	Limiting Ionic Conductivity
$\mu$	Dynamic Viscosity
$\mu_i^0$	Standard Chemical Potential
$\phi$	Electric potential
$\text{p}K_a$	Logarithmic Acid Dissociation Constant
$a$	Activity
$D$	Diffusion Coefficient
$I$	Current Density
$j$	Ion Flux Density
$P$	Pressure
$T$	Absolute temperature
$V$	Volume
$z$	Ion Charge Number

# Bibliography

- [1] S. ABDU, M. C. MARTÍ-CALATAYUD, J. E. WONG, M. GARCÍA-GABALDÓN, AND M. WESSLING, *Layer-by-layer modification of cation exchange membranes controls ion selectivity and water splitting*, ACS Applied Materials and Interfaces, 6 (2014), pp. 1843–1854.
- [2] P. ATKINS AND J. PAULA, *Physical chemistry*, W.H. Freeman, 2006.
- [3] A. BARD AND L. FAULKNER, *Electrochemical Methods: Fundamentals and Applications*, wiley, 2002.
- [4] E. BARSOUKOV AND J. R. MACDONALD, *Impedance Spectroscopy: Theory, Experiment, and Applications*, Wiley, 2005.
- [5] Z. CAO, P. I. GORDIICHUK, K. LOOS, E. J. R. SUDHÖLTER, AND L. C. P. M. DE SMET, *The effect of guanidinium functionalization on the structural properties and anion affinity of polyelectrolyte multilayers*, Soft Matter, 12 (2016), pp. 1496–1505.
- [6] A. CHAPOTOT, G. POURCELLY, AND C. GAVACH, *Transport competition between monovalent and divalent cations through cation-exchange membranes. Exchange isotherms and kinetic concepts*, Journal of Membrane Science, 96 (1994), pp. 167–181.
- [7] J. H. CHOI, J. S. PARK, AND S. H. MOON, *Direct measurement of concentration distribution within the boundary layer of an ion-exchange membrane*, Journal of Colloid and Interface Science, 251 (2002), pp. 311–317.
- [8] D. CORDELL, J. O. DRANGERT, AND S. WHITE, *The story of phosphorus: Global food security and food for thought*, Global Environmental Change, 19 (2009), pp. 292–305.
- [9] E. L. CUSSLER, *Diffusion : Mass Transfer in Fluid Systems*, Cambridge University Press, 2009.
- [10] G. DECHER, J. D. HONG, AND J. SCHMITT, *Buildup of ultrathin multilayer films by a self-assembly process: III. Consecutively alternating adsorption of anionic and cationic polyelectrolytes on charged surfaces*, Thin Solid Films, 210-211 (1992), pp. 831–835.

- [11] P. DŁUGOLECKI, P. OGOŃSKI, S. J. METZ, M. SAAKES, K. NIJMEIJER, AND M. WESSLING, *On the resistances of membrane, diffusion boundary layer and double layer in ion exchange membrane transport*, Journal of Membrane Science, 349 (2010), pp. 369–379.
- [12] F. DONNAN, *Die genaue thermodynamik der membranegleichgewichte*, Z. Phys. Chem. A, 168 (1934), pp. 369–380.
- [13] EIDGENÖSSISCHES DEPARTEMENT FÜR UVEK, *Totalrevision der Technischen Verordnung über Abfälle (TVA)*, Tech. Rep. O342-0454, Swiss Government, Bern, Switzerland, 2015.
- [14] M. J. ESHLAGHI, *Permselectivity and Electrical Resistance of Anion Exchange Membranes: Correlation between process parameters and membrane performance for phosphate removal*, PhD thesis, TU Delft, 2016.
- [15] EUROPEAN COMMISSION, *Critical Raw Materials - European Commission*, 2017.
- [16] R. FEMMER, A. MANI, AND M. WESSLING, *Ion transport through electrolyte/polyelectrolyte multi-layers*, Scientific Reports, 5 (2015), p. 11583.
- [17] E. FONTANANOVA, W. ZHANG, I. NICOTERA, C. SIMARI, W. VAN BAAK, G. DI PROFIO, E. CURCIO, AND E. DRIOLI, *Probing membrane and interface properties in concentrated electrolyte solutions*, Journal of Membrane Science, 459 (2014), pp. 177–189.
- [18] D. R. FRANCESCHETTI AND J. R. MACDONALD, *Electrode kinetics, equivalent circuits, and system characterization: Small-signal conditions*, Journal of Electroanalytical Chemistry and Interfacial Electrochemistry, 82 (1977), pp. 271–301.
- [19] A. H. GALAMA, N. A. HOOG, AND D. R. YNTEMA, *Method for determining ion exchange membrane resistance for electrodialysis systems*, Desalination, 380 (2016), pp. 1–11.
- [20] A. H. GALAMA, D. A. VERMAAS, J. VEERMAN, M. SAAKES, H. H. M. RIJNAARTS, J. W. POST, AND K. NIJMEIJER, *Membrane resistance: The effect of salinity gradients over a cation exchange membrane*, Journal of Membrane Science, 467 (2014), pp. 279–291.

- [21] J. GRANTHAM, *Be persuasive. Be brave. Be arrested (if necessary).*, Nature, 491 (2012), p. 303.
- [22] F. GUESMI, C. HANNACHI, AND B. HAMROUNI, *Selectivity of anion exchange membrane modified with polyethyleneimine*, Ionics, 18 (2012), pp. 711–717.
- [23] E. GÜLER, W. VAN BAAK, M. SAAKES, AND K. NIJMEIJER, *Monovalent-ion-selective membranes for reverse electrodialysis*, Journal of Membrane Science, 455 (2014), pp. 254–270.
- [24] D. JOHNSON, *Zview 2*, 2010.
- [25] N. JOSEPH, P. AHMADIANNAMINI, R. HOOGENBOOM, AND I. F. J. VANKELECOM, *Layer-by-layer preparation of polyelectrolyte multilayer membranes for separation*, Polym. Chem., 5 (2014), pp. 1817–1831.
- [26] W. JUDA, *Coherent ion-exchange gels and membranes*, Journal of the American Chemical Society, 72 (1950), p. 1044.
- [27] KAARINA SCHENK, *Phosphorous in Switzerland Material flows, targets, options, P-recovery*, in World Resources Forum, World Resources Forum, 2009.
- [28] A. E. KOZMAI, V. V. NIKONENKO, N. D. PISMENSKAYA, S. A. MAREEV, E. I. BELOVA, AND P. SISTAT, *Use of electrochemical impedance spectroscopy for determining the diffusion layer thickness at the surface of ion-exchange membranes*, Petroleum Chemistry, 52 (2013), pp. 614–624.
- [29] J. J. KROL, M. WESSLING, AND H. STRATHMANN, *Concentration polarization with monopolar ion exchange membranes: Current-voltage curves and water dissociation*, Journal of Membrane Science, 162 (1999), pp. 145–154.
- [30] M. L. PALTRINIERI, E. J. S. WANG, S. SACHDEVA, N. A. M. BESSELING, AND L. DE SMET, *Fe<sub>3</sub>O<sub>4</sub> nanoparticles coated with a guanidinium-functionalized polyelectrolyte extend the pH range for phosphate binding*, Journal of Materials Chemistry A, (2017).
- [31] E. LEVLIN, *Recovery of Phosphate From Sewage Sludge and Separation of Metals By Ion Exchange*, Land and Water Resources Engineering, 3 (1995), pp. 1–12.

- [32] S. R. LEWIS, S. DATTA, M. GUI, E. L. COKER, F. E. HUGGINS, S. DAUNERT, L. BACHAS, AND D. BHATTACHARYYA, *Reactive nanostructured membranes for water purification*, Proc Natl Acad Sci U S A, 108 (2011), pp. 8577–8582.
- [33] R. LI, J. J. WANG, B. ZHOU, M. K. AWASTHI, A. ALI, Z. ZHANG, A. H. LAHORI, AND A. MAHAR, *Recovery of phosphate from aqueous solution by magnesium oxide decorated magnetic biochar and its potential as phosphate-based fertilizer substitute*, Bioresource Technology, 215 (2016), pp. 209–214.
- [34] D. R. LIDE, *CRC Handbook of Chemistry and Physics, 84th Edition, 2003-2004*, Handbook of Chemistry and Physics, 53 (2003), p. 2616.
- [35] B. E. LOGAN AND M. ELIMELECH, *Membrane-based processes for sustainable power generation using water*, Nature, 488 (2012), pp. 313–319.
- [36] D. D. MACDONALD, *Reflections on the history of electrochemical impedance spectroscopy*, Electrochimica Acta, 51 (2006), pp. 1376–1388.
- [37] MATHWORKS, *MATLAB 2016a*, 2016.
- [38] G. MERLE, M. WESSLING, AND K. NIJMEIJER, *Anion exchange membranes for alkaline fuel cells: A review*, 2011.
- [39] METROHM, *Nova 1.11*, 2017.
- [40] MINISTERIE VAN VERKEER EN WATERSTAAT, *Vierde Nota Waterhuishouding Regeringsbeslissing*, Tech. Rep. Z42-a44, Dutch Government, The Hague, Netherlands, 1998.
- [41] A. A. MOYA, *Electric circuits modelling the low-frequency impedance of ideal ion-exchange membrane systems*, Electrochimica Acta, 62 (2012), pp. 296–304.
- [42] —, *Electrochemical impedance of ion-exchange membranes in ternary solutions with two counterions*, Journal of Physical Chemistry C, 118 (2014), pp. 2539–2553.
- [43] —, *Electrochemical Impedance of Ion-Exchange Membranes with Interfacial Charge Transfer Resistances*, The Journal of Physical Chemistry C, 120 (2016), pp. 6543–6552.
- [44] M. MUDLER, *Basic principles of membrane technology*, Kluwer Academic Publishers, Dordrecht, Netherlands, 1996.

- [45] V. V. NIKONENKO AND A. E. KOZMAI, *Electrical equivalent circuit of an ion-exchange membrane system*, *Electrochimica Acta*, 56 (2011), pp. 1262–1269.
- [46] J.-S. PARK, J.-H. CHOI, J.-J. WOO, AND S.-H. MOON, *An electrical impedance spectroscopic (EIS) study on transport characteristics of ion-exchange membrane systems*, *Journal of Colloid and Interface Science*, 300 (2006), pp. 655–662.
- [47] A. PEERS, *General Discussion*, *Disc Faraday Soc*, 21 (1956), pp. 124–125.
- [48] G. QIU AND Y. P. TING, *Direct phosphorus recovery from municipal wastewater via osmotic membrane bioreactor (OMBR) for wastewater treatment*, *Biore-source Technology*, 170 (2014), pp. 221–229.
- [49] V. SARAPULOVA, E. NEVAKSHENOVA, N. PISMENSKAYA, L. DAMMAK, AND V. NIKONENKO, *Unusual concentration dependence of ion-exchange membrane conductivity in ampholyte-containing solutions: Effect of ampholyte nature*, *Journal of Membrane Science*, 479 (2015), pp. 28–38.
- [50] P. SISTAT, A. KOZMAI, N. PISMENSKAYA, C. LARCHET, G. POURCELLY, AND V. NIKONENKO, *Low-frequency impedance of an ion-exchange membrane system*, *Electrochimica Acta*, 53 (2008), pp. 6380–6390.
- [51] V. SMIL, *Phosphorus in the environment: Natural Flows and Human Interferences*, *Annual Review of Energy and the Environment*, 25 (2000), pp. 53–88.
- [52] H. STRATHMANN, *Electrodialysis, a mature technology with a multitude of new applications*, *Desalination*, 264 (2010), pp. 268–288.
- [53] Y. TANAKA, *Ion Exchange Membranes*, Elsevier, 2015.
- [54] M. VASELBEHAGH, H. KARKHANECHI, R. TAKAGI, AND H. MATSUYAMA, *Surface modification of an anion exchange membrane to improve the selectivity for monovalent anions in electrodialysis - experimental verification of theoretical predictions*, *Journal of Membrane Science*, 490 (2015), pp. 301–310.
- [55] D. A. VERMAAS, M. SAAKES, AND K. NIJMEIJER, *Enhanced mixing in the diffusive boundary layer for energy generation in reverse electrodialysis*, *Journal of Membrane Science*, 453 (2014), pp. 312–319.

- [56] Y. YE, H. H. NGO, W. GUO, Y. LIU, X. ZHANG, J. GUO, B. JIE NI, S. W. CHANG, AND D. D. NGUYEN, *Insight into biological phosphate recovery from sewage*, *Bioresource Technology*, 218 (2016), pp. 874–881.
- [57] W. ZHANG, J. MA, P. WANG, Z. WANG, F. SHI, AND H. LIU, *Investigations on the interfacial capacitance and the diffusion boundary layer thickness of ion exchange membrane using electrochemical impedance spectroscopy*, *Journal of Membrane Science*, 502 (2016), pp. 37–47.
- [58] Y. ZHANG, E. DESMIDT, A. VAN LOOVEREN, L. PINOY, B. MEESCHAERT, AND B. VAN DER BRUGGEN, *Phosphate separation and recovery from wastewater by novel electrodialysis*, *Environmental Science and Technology*, 47 (2013), pp. 5888–5895.